AMERICAN SOCIETY FOR MICROBIOLOGY | Applied and Environmental Microbiology®

ENVIRONMENTAL MICROBIOLOGY

Transcriptomic Analysis of the Dual Response of *Rhodococcus aetherivorans* BCP1 to Inorganic Arsenic Oxyanions

A. Firrincieli,[a] D. Zannoni,[a] E. Donini,[a] H. Dostálová,[b] R. Rädisch,[b] L. Iommarini,[a] R. J. Turner,[c] T. Busche,[d] M. Pátek,[b] M. Cappelletti[a]

[a]Department of Pharmacy and Biotechnology, University of Bologna, Bologna, Italy
[b]Institute of Microbiology of the Czech Academy of Sciences, Prague, Czech Republic
[c]Department of Biological Sciences, University of Calgary, Calgary, Canada
[d]Center for Biotechnology, Bielefeld, Germany

ABSTRACT Bacterial strains belonging to the genus *Rhodococcus* are able to degrade various toxic organic compounds and tolerate high concentrations of metal (loid)s. We have previously shown that *Rhodococcus aetherivorans* BCP1 is resistant to various levels of the two arsenic inorganic species, arsenite [As(III)] and arsenate [As(V)]. However, while arsenite showed toxic effects at concentrations as low as 5 mM, arsenate at 30 mM boosted the growth rate of BCP1 cells and was toxic only at concentrations of >100 mM. Since such behavior could be linked to peculiar aspects of its metabolism, the transcriptomic analysis of BCP1 cells exposed to 5 mM As(III) and 30 mM As(V) was performed in this work. The aim was to clarify the mechanisms underlying the arsenic stress response of the two growth phenotypes in the presence of the two different oxyanions. The results revealed that As(III) induced higher activity of reactive oxygen species (ROS)-scavenging enzymes than As(V) in relation to the expression of enzymes involved in cellular damage recovery and redox buffers/cofactors (ergothioneine, mycofactocin, and mycothiol). Further, As(III) downregulated pathways related to cell division, while both oxyanions downregulated genes involved in glycolysis. Notably, As(V) induced the expression of enzymes participating in the synthesis of metallophores and rearranged the central and energetic metabolism, also inducing alternative pathways for ATP synthesis and glucose consumption. This study, in providing transcriptomic data on *R. aetherivorans* exposed to arsenic oxyanions, sheds some light on the plasticity of the rhodococcal response to arsenic stress, which may be important for the improvement of biotechnological applications.

IMPORTANCE Members of the genus *Rhodococcus* show high metabolic versatility and the ability to tolerate/resist numerous stress conditions, including toxic metals. *R. aetherivorans* BCP1 is able to tolerate high concentrations of the two inorganic arsenic oxyanions, arsenite [As(III)] and arsenate [As(V)]. Despite the fact that BCP1 intracellularly converts As(V) into As(III), this strain responds very differently to the presence of these two oxyanions in terms of cell growth and toxic effects. Indeed, while As(III) is highly toxic, exposure to specific concentrations of As(V) seems to boost cell growth. In this work, we investigated the transcriptomic response, ATP synthesis, glucose consumption, and H_2O_2 degradation in BCP1 cells exposed to As(III) and As(V), inducing two different growth phenotypes. Our results give an overview of the transcriptional rearrangements associated with the dual response of BCP1 to the two oxyanions and provide novel insights into the energetic metabolism of *Rhodococcus* under arsenic stress.

KEYWORDS *Rhodococcus*, arsenic resistance, bacterial stress response, oxidative stress, transcriptomics, mycothiol, ergothioneine, oxidative phosphorylation

Editor Maia Kivisaar, University of Tartu

Address correspondence to M. Cappelletti, martina.cappelletti2@unibo.it.

The authors declare no conflict of interest.

Received 10 November 2021
Accepted 11 February 2022

Arsenic is considered one of the most pervasive toxic metalloids, ranking first on the U.S. Environmental Protection Agency's Superfund List. It originates primarily from the natural weathering of the earth's crust and is ubiquitous in the environment. Anthropogenic sources of contamination can also be significant, especially in areas with mining activity and industrial arsenic applications (1). Depending on the environmental conditions, arsenic exists in different inorganic and organic species. The most common are the inorganics, namely, the trivalent species, As(III), i.e., the oxyanion arsenite (AsO^{2-}), and the pentavalent species, As(V), or arsenate (AsO_4^{3-}), followed by the organic arsenic compounds presenting methyl groups. The toxicity of As(III) is mainly associated with its interaction with sulfhydryl (SH) groups of proteins, which, because of this binding, are altered in their conformation and function (2). Conversely, As(V) is a molecular analog of phosphate (HPO_4^{2-}) which can compete for phosphate anion transporters and replace phosphate in some biochemical reactions (2). For instance, the inhibition of ATP generation during oxidative phosphorylation due to the replacement of phosphate with arsenate has been described (2). The replacement of phosphate by arsenic in DNA was also reported, although this aspect remains strongly debated and was finally disproved (2). Interconversion of the different arsenic species also occurs in nature with the participation of microorganisms, influencing the mobilization and availability of arsenic in the environment (3).

Because bacteria have been exposed to arsenic since their origin, they have evolved several strategies to deal with its toxicity. In a few cases, inorganic arsenic can be part of the energetic metabolism and be utilized as a final electron acceptor or as an energy source. However, more generally, bacteria are not able to use As(V) and As(III) for energetic purposes and exploit specific detoxification mechanisms, which typically involve reduction or oxidation reactions combined with export processes (4, 5).

Bacterial strains belonging to the genus *Rhodococcus* were characterized by the resistance to stresses caused by various compounds and extreme conditions that makes them a suitable candidate for biotechnology applications in both bioremediation and bioconversion/biosynthesis processes (6–10). Recently, some papers reported the extraordinary resistance of rhodococci to toxic metal(loid)s (e.g., tellurium, selenium and arsenic), which for a long time was mostly associated with the nature of the mycolate cell wall (11–13). The first indications of specific genetic determinants associated with metal resistance in *Rhodococcus* were reported (9, 14). In particular, arsenate [As(V)] was found to transcriptionally induce the *ars* gene cluster in *Rhodococcus aetherivorans* strain BCP1, which is characterized by hypertolerance to toxic organic and inorganic compounds (9, 14–17). The *ars* gene cluster codes for different arsenate reductases which contribute to BCP1 resistance to arsenic by intracellularly reducing As(V) to As(III), which in turn can be extruded by the efflux pump Acr3-ArsA (14). In addition to inducing genetic determinants which encode enzymes involved in metal resistance mechanisms, metal(loid)s can also induce genes that are involved in general and specific stress responses. This can contribute to the overall high resistance capacities of *Rhodococcus* cells. While these stress response mechanisms in *Rhodococcus* still have not been adequately described from a genetic and molecular point of view (10), the taxonomically related genus *Mycobacterium* has been quite extensively studied in this regard, mostly in relation to its pathogenic lifestyle. The stress response in bacteria is regulated by transcriptional regulators, two-component systems, and sigma factors of RNA polymerase. It is known that a complex sigma factor network responds to various stress conditions (10) and that extracytoplasmic function (ECF) sigma factors (group 4) have a prominent role in stress response. The activity of ECF sigma factors was investigated in detail in the related organisms *Mycobacterium* and *Corynebacterium* but only superficially in *Rhodococcus*.

In this work, we analyzed the global transcriptional response of *Rhodococcus aetherivorans* BCP1 cells exposed to either As(III) or As(V) in order to get molecular insight into their response to these toxic metalloids and the plasticity of the stress response. In this respect, the transcriptional profile underlying the apparent improved growth performance previously observed in As(V)-exposed cells was compared with the transcriptional response of BCP1 cells exposed to a subinhibitory concentration of As(III). As a result, several genes involved in oxidative stress response, redox homeostasis, and central and bioenergetic metabolism were found to be

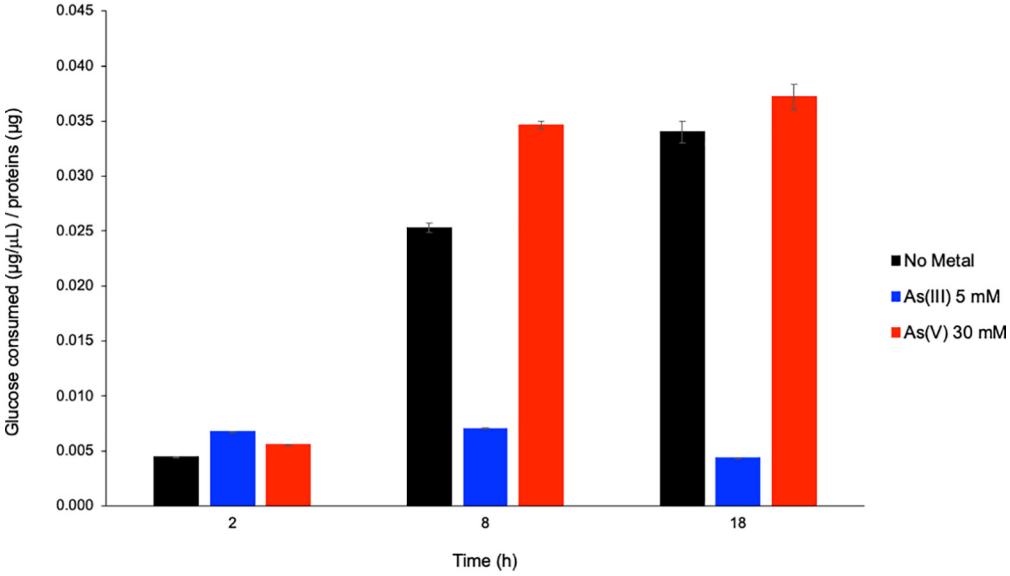

FIG 1 Glucose consumption of *R. aetherivorans* BCP1 cells exposed to As(III) (5 mM) and As(V) (30 mM). The glucose consumed was measured after 2, 8, and 18 h of cell treatment with As(III), As (V), or no metal (untreated cells) compared to the amount of glucose present at the time of initial exposure and normalized to the total amount of protein. Plotted values are averages and standard deviations for two independent biological replicates.

differentially expressed upon exposure to these arsenic species. These transcriptional results were further supported by some experimental evidence on cell growth, glucose consumption, reactive oxygen species (ROS) detoxification system activity, and ATP synthesis.

RESULTS

Determination of glucose consumption and the amount of endogenous ATP in cell cultures of *R. aetherivorans* BCP1 exposed to subinhibitory concentrations of As(III) and As(V). It was shown previously that *R. aetherivorans* BCP1 cultivated in M9 medium with 0.2% glucose is resistant to millimolar amounts of arsenic, showing different growth phenotypes on 5 mM As(III) (arsenite) versus 30 mM As(V) (arsenate) (14). Indeed, BCP1 cells initially inoculated at 5 $\log_{10}$ CFU mL^{-1} grew in up to 8 mM As(III), whereas their growth performance was slightly improved in the presence of 30 mM As(V) within an exposure time range of 6 to 24 h (14). To further investigate these previous results, we monitored the glucose consumption and ATP intracellular amount in parallel with the growth of *R. aetherivorans* BCP1 cells during their exposure to subinhibitory concentrations of 5 mM As(III) and 30 mM As(V) compared to control (untreated) cells. As shown in Fig. 1, glucose consumption increased in both untreated cells and cells exposed to As(V) from time 1 (2 h) to time 2 (8 h). Then, the consumption slightly increased in between 8 h and the 18 h of exposure, although to a lower extent, most likely due to the entrance of the cells into stationary phase. Conversely, the exposure of the cells to As(III) stalled the increase of glucose consumption, which remained constant over the analyzed time period.

With regard to ATP production in relation to the cell growth, the addition of 5 mM As(III) decreased the cytosolic ATP levels approximately 40% (±2%) without affecting the initial cell growth kinetics (from time zero to time 1 [2 h]) (Fig. 2A and B). In contrast, 30 mM As (V) not only did not alter the growth of the cells at time 1 (Fig. 2B) but, similarly to the control, increased the endogenous pool of ATP by 50% (±10%) (Fig. 2A). Further, in cells exposed to As(III) the decrease in endogenous ATP persisted through time 2 (after 8 h) and time 3 (after 18 h), while a significant decrease of the ATP endogenous pool was observed (with respect to time zero) in both control cells and cells treated with As(V) only after 18 h, i.e., during the stationary growth phase. These results reinforce the previous data reported by Firrincieli et al. (14) regarding the different effects of As(III) and As(V) on the growth phenotype of BCP1 by revealing that the patterns of the glucose consumption and endogenous

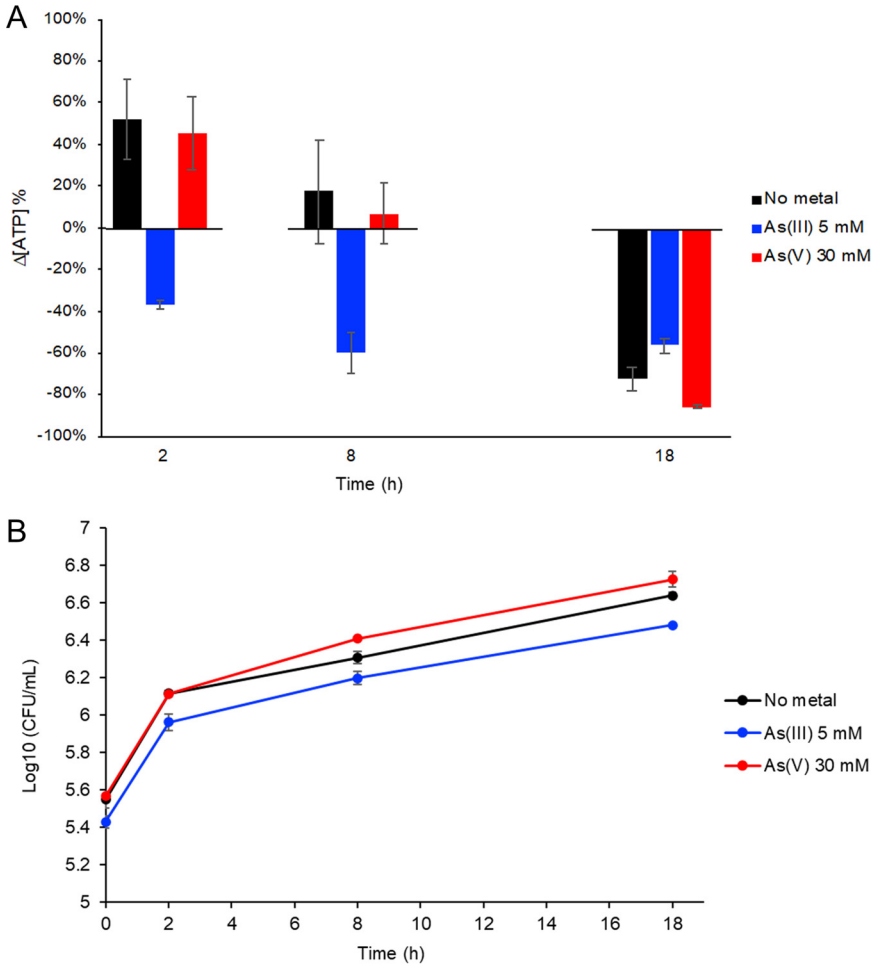

FIG 2 Variation in intracellular ATP levels (A) and growth curve (B) in the presence or absence (no metal) of arsenic [As(III) (5 mM) or As(V) (30 mM)]. The intracellular ATP variations (nM μg proteins^{-1}) are expressed as the percent variance in ATP concentration (Δ[ATP]%) measured after 2, 8, or 18 h of exposure over the corresponding ATP level measured at time zero. Plotted values per condition are averages and standard deviations for three independent biological replicates.

pool of ATP are similar in control (untreated) cells and cells exposed to 30 mM As(V). Conversely, the presence of As(III) negatively affected the glucose consumption and altered the intracellular ATP pool production over the time period analyzed.

Overview of the DEGs in As(V) and As(III) and their functional categories. Transcriptomic analysis (RNA-seq) of *R. aetherivorans* BCP1 cells exposed to arsenic oxyanions yielded 437 and 518 differentially expressed genes (DEGs) in the presence of 5 mM As(III) and 30 mM As(V), respectively (Fig. 3). Of them, 171 genes were upregulated and 266 genes were downregulated in response to As(III), whereas 71 and 447 genes were down- and upregulated, respectively, in response to As(V) (Fig. 3C; also, see Table S1 in the supplemental material). Only 7.6% of all DEGs were shared between the transcriptional patterns of BCP1 cells exposed to As(III) and As(V), and these did not include the top 10 up- and downregulated genes in each arsenic species (see Fig. S1 in the supplemental material). Ten randomly selected DEGs representing different functional categories were analyzed through quantitative real-time PCR (qRT-PCR) analysis (Fig. S2). The $\log_2$ fold change in expression of the selected genes indicates a general agreement between RT-qPCR and RNA-seq data in capturing expression changes (Fig. S2).

The overview of the functional categories of DEGs showed that As(III)-upregulated genes are mainly involved in oxidation-reduction processes (GO:0055114) and response to cadmium (GO:0046686), whereas As(III)-downregulated genes are related to cellular growth (GO:0040007), translation (GO:0042255 and GO:0017148) and posttranslational modifications

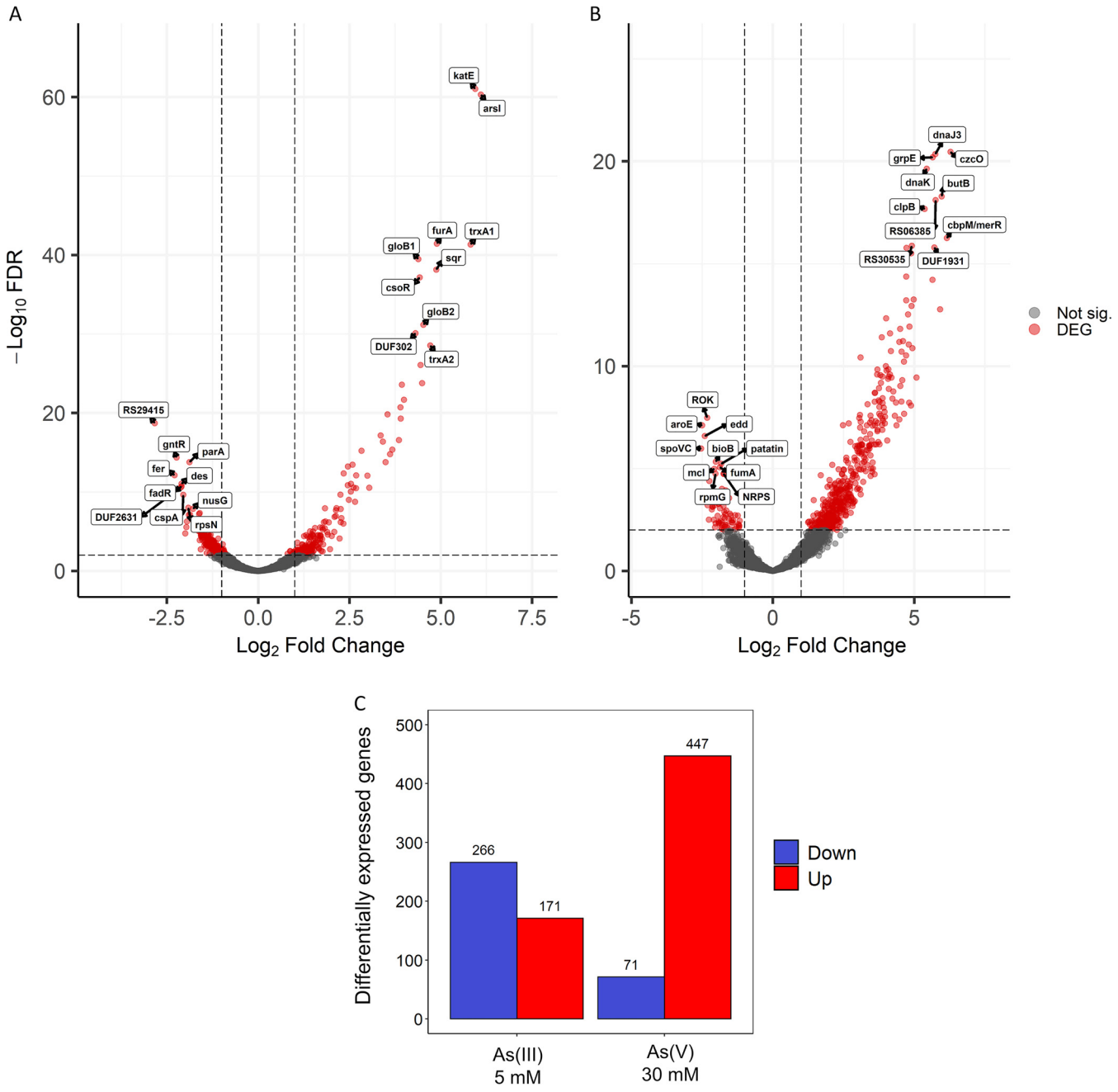

FIG 3 Differentially expressed genes (DEGs) in *R. aetherivorans* BCP1 exposed to As(III) (5 mM) and As(V) (30 mM). (A and B) Volcano plot of BCP1 cells exposed to 5 mM As(III) (A) or 30 mM As(V) (B) compared to the control (i.e., absence of metal). Gene names for the top 10 up- and downregulated DEGs (with the lowest FDR) are in black boxes. (C) Bar plot of up- and downregulated genes in As(III)- or As(V)-exposed cells compared to the control (i.e., absence of metal). Only genes having an FDR of <0.01 are plotted.

(GO:0071822), and synthesis of organonitrogen compounds (GO:1901566) (Table 1; Table S2). As(V) upregulated genes significantly associated with nitrosative and oxidative stresses (GO:0051409 and GO:0042744), synthesis of ergothioneine (GO:0052704), cellular respiration (GO:0036293 and GO:0045333), and response to unfolded proteins (GO:0019941), while As (V)-downregulated genes are related to the biosynthesis of biotin (GO:0009102) and amino acids associated with diaminopimelate biosynthesis (GO:0019877) (Table 1; Table S2). By analyzing the 10 most upregulated genes in response to each arsenic species, we observed that those strongly upregulated in As(III) are related to ROS scavenging systems (i.e., *trx*, *katE*, and *furA*) (Fig. 3A). Those overexpressed by As(V) are associated with the response to protein damage/aggregation (i.e., *dnaJ3*, *dnaK*, *clpB*, *grpE*, and *cbpM/merR*) (Fig. 3B).

TABLE 1 Functional categories significantly up- or downregulated by 5 mM As(III) and/or 30 mM As(V) in *R. aetherivorans* BCP1[a]

As species	Regulation	GO ID	GO term	No. of genes		*P* value
				Annotated	Significant	
As(III)	Up	GO:0055114	Oxidation-reduction process	166	11	0.00018
		GO:0046686	Response to cadmium ion	2	2	0.00044
	Down	GO:1901566	Organonitrogen compound biosynthetic process	266	46	0.0026
		GO:0042255	Ribosome assembly	34	10	0.0034
		GO:0071822	Protein complex subunit organization	37	10	0.0066
		GO:0040007	Growth	393	58	0.0072
		GO:0017148	Negative regulation of translation	8	4	0.0082
As(V)	Up	GO:0035690	Cellular response to drug	6	4	0.00047
		GO:0019941	Modification-dependent protein catabolic process	5	3	0.00419
		GO:0036293	Response to decreased oxygen levels	22	6	0.00528
		GO:0052704	Ergothioneine biosynthesis from histidine via gamma-glutamyl-hercynylcysteine sulfoxide	2	2	0.00612
		GO:0042744	Hydrogen peroxide catabolic process	2	2	0.00612
		GO:0045333	Cellular respiration	23	6	0.0067
		GO:0051409	Response to nitrosative stress	11	4	0.00767
	Down	GO:0009102	Biotin biosynthetic process	5	3	0.0002
		GO:0019877	Diaminopimelate biosynthetic process	3	2	0.0023

[a]Details of the gene accession numbers and gene functional annotation are in Table S2.

Description of the DEGs associated with BCP1 response to As(III) and As(V). (i) Stress response. The cells afflicted by toxic stressors naturally activate the enzymes, which can degrade or detoxify the compounds that are the sources of the chemostress. Regarding the genetic determinants of arsenic detoxification, the *ars* gene cluster is organized in two divergent transcriptional units in the BCP1 genome (14). Transcription of all these genes was induced in response to both arsenic species, although the transcription levels were significant only in As(III)-exposed cells (Fig. 4; Table S3). Conversely, the *arsI* gene, encoding the carbon-As lyase that degrades methylarsenite [MAs(III)] to As(III) and formaldehyde, not only was significantly overexpressed in the presence of both As(III) and As(V) but also was identified as one of the most upregulated genes in As(III)-exposed cells (Fig. 3A).

The two arsenic species induced the expression of catalase genes (*kat*) and the nitric oxide dioxygenase gene (*nod*), which are involved in the detoxification of reactive oxygen and nitrogen species (ROS and RNS, respectively) (Fig. 4; Table S3). Regarding the genes encoding ROS-detoxifying enzymes, As(III) upregulated a gene cluster including *katE*, the ferric uptake regulator (*fur*) gene, and *dps*, which codes for a starvation-inducible DNA-binding protein. Conversely, As(V) upregulated a different *fur* gene together with the flanking catalase-peroxidase gene (*katG*) and a distinct *katE* homolog that is located immediately downstream of a gene encoding the FisR family transcriptional regulator AcoR. This regulatory protein possesses the c-di-GMP binding domain GAF and was described as being involved in acetoin/glycerol metabolism.

As to the genes encoding RNS-detoxifying enzymes (*nod*), the As(III)-responsive gene *nod2* was upregulated together with the downstream nitric oxide-sensitive transcription regulator gene (*nsr2*). This is a global regulator which is involved in the expression of stress-related gene regulons and in *Actinobacteria* seems to control both nitric oxide-specific and general stress responses (18). In contrast, As(V)-responsive *nod1* was upregulated as a monocistronic gene that was separate from any regulatory gene on the chromosome.

Many other genes induced by both the arsenic oxyanions are apparently connected to oxidative stress. As(III) upregulated the gene cluster *oxyR-ahpFC-nemA*, which codes for the regulatory protein OxyR, the alkyl hydroperoxide reductase Ahp, which reduces organic peroxides to repair cellular targets (e.g., fatty acids and DNA), and the *N*-ethylmaleimide reductase Nem, involved in the degradation of toxic nitrous compounds, such as *N*-ethylmaleimide (NEM) (Fig. 4; Table S3). Additionally, As(III) upregulated the genes encoding (i) the methionine sulfoxide reductases MsrA and MsrB, which catalyze the reduction of oxidized methionine; (ii) the genes encoding rhodanese-like proteins,

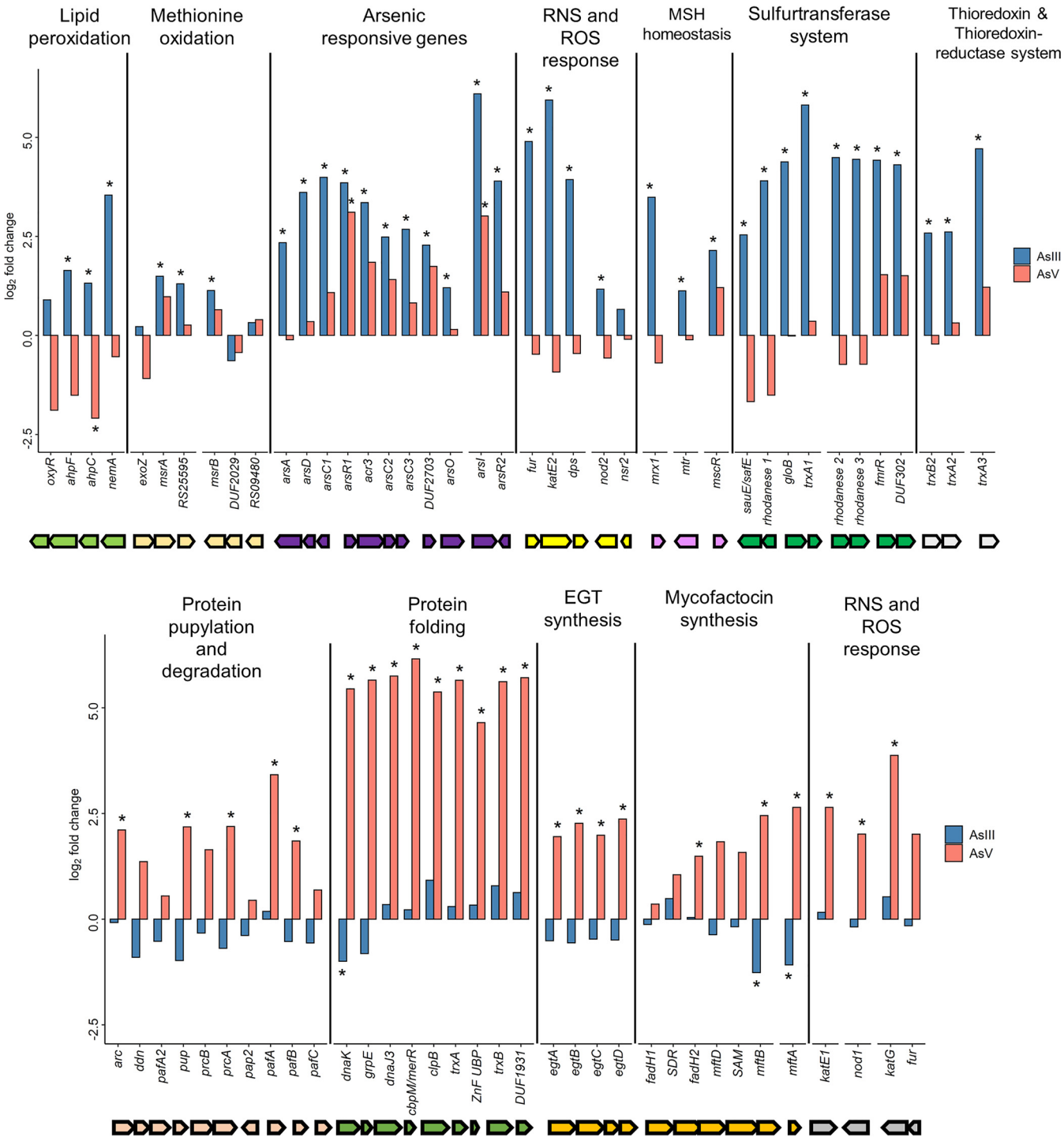

FIG 4 Stress response-related genes and gene clusters differentially expressed in *R. aetherivorans* BCP1 exposed to 5 mM As(III) or 30 mM As(V). Asterisks indicate statistically significant differences in the gene expression levels detected in As(III)- and As(V)-exposed BCP1 cells compared to the control condition (i.e., absence of metal). Genes coding for hypothetical proteins are named after the gene locus tag. Raw data used for the bar plots are reported in Table S3. KEGG Orthology (KO) annotation of the genes is reported in Table S1. Breaks in the x-axis indicate that the genes are not contiguous in the genome.

acting as sulfurtransferases, which are possibly involved in regenerating intracellular thiols (19); and (iii) the thioredoxin thioredoxin-reductase genes encoding TrxA and TrxB.

An additional difference between As(V)- and As(III)-grown cells concerned the differential expression of genes that control the intracellular levels of the two major redox buffers, ergothioneine (EGT) and mycothiol (MSH). Indeed, DEG analysis showed that *mrx* (mycoredoxin),

TABLE 2 Sigma factor- and anti-sigma factor-coding genes differentially expressed in BCP1 cells exposed to "As(III) and As(V)"

		As(III)		As(V)	
Locus tag	Gene	Log_2 fold change[a]	FDR	Log_2 fold change[a]	FDR
RS13120	*sigZ*	1.68	1.07E−04	−0.3	NA[b]
RS14335	*rshA*[c]	2.33	1.02E−06	0.99	0.34
RS14340	*sigH*	1.39	2.16E−04	0.92	0.21
RS20780	*sigG*	0.76	3.58E−02	2	1.49E−03
RS09290	*sigA*	−1.04	5.30E−03	0.42	0.67

[a]Relative to the control.
[b]NA, not applicable.
[c]Gene encoding the anti-sigma factor of SigH.

mtr (mycothione reductase), and the *sigH-rshA* system, which control the intracellular levels of reduced MSH, are significantly overexpressed only in As(III)-grown cells (Fig. 4, Table 2; Table S3). On the other hand, the exposure to As(V) upregulated the genes *egtABCD*, which drive the biosynthesis of EGT, i.e., a sulfur-containing derivative of the amino acid histidine with potent antioxidant activities (20).

As(V) upregulated operons encoding the ATP-powered protein chaperones DnaK and ClpB and the cofactor DnaJ3, involved in the recovery of protein aggregates (21) and gene operons including *pup*, *arc*, *prc*, and *paf*, which are involved in the posttranslational protein pupylation process and protein degradation (22).

Several oxidoreductases belonging to oxygenase and dehydrogenase categories and involved in hydrocarbon oxidation and xenobiotic cometabolism were also induced by As(V), such as catechol and benzoate dioxygenases and soluble di-iron monooxygenases (Prm and Smo) (23, 24) (Table S1).

To corroborate the transcriptomic data on the DEGs involved in ROS detoxification, the capacity of As(III)- and As(V)-exposed cells to scavenge H_2O_2 was assayed. As a result, in untreated BCP1 cells (control), 54.5% (±2.4%) of the initial amount of added H_2O_2 was detected in the reaction assay after 30 min of incubation. Conversely, by testing As (III)- and As(V)-exposed cells, the remaining H_2O_2 in the reaction assay was 27.6% (±2.5%) and 39.4% (±6.8%), respectively. These results indicate that cells exposed to both As(III) and As(V) can decompose more H_2O_2 than control cells, although the As(III)-exposed cells have the most efficient ROS detoxification systems.

(ii) Putative sigma factors. Based on the amino acid sequences of sigma factors deduced from the *sig* genes of *Mycobacterium* and *Rhodococcus* species, we found 12 *sig* genes—*sigA*, *sigB*, *sigD*, *sigE*, *sigF*, *sigG*, *sigH* (homologous to *sigR* in *Streptomyces*), *sigI*, *sigJ*, *sigK*, *sigM*, and *sigZ*—in the *R. aetherivorans* BCP1 genome (Table S4). Transcriptional patterns of BCP1 cells obtained in this work showed that As(V) significantly upregulated *sigG*, while As (III) induced the overexpression of *sigH* with the corresponding anti-sigma factor gene *rshA* and *sigZ* (Table 2). As(III) also downregulated *sigA*. While SigA is a vegetative sigma factor, SigG, SigH, and SigZ are alternative sigma factors typically involved in stress response.

(iii) Central metabolism. The two arsenic oxyanions differently regulated BCP1 genes involved in central metabolism, energy production, and cell growth and division.

As(III) strongly inhibited the genes involved in the two major glucose consumption pathways in *Rhodococcus*, i.e., the Entner-Doudoroff pathway (EDP) and the Embden-Meyerhof-Parnas (EMP) pathway. These genes were also downregulated in the presence of As(V), but to a lower extent (Fig. 5; Table S5), with the exception of phosphoenolpyruvate synthase (*pps*). The EDP genes *edd* (phosphogluconate dehydratase) and *eda* (2-dehydro-3-deoxy-phosphogluconate aldolase) were significantly downregulated in the presence of both As(V) and As(III). Similarly, several genes involved in the EMP pathway, namely, *pgi* (glucose 6-phosphate isomerase), *gap* (glyceraldehyde 3-phosphate dehydrogenase), *gpm* (phosphoglycerate mutase), *eno* (enolase), *glk* (glucose kinase) and *pyk* (pyruvate kinase), were downregulated by both the arsenic species (Fig. 5; Table S5). Nevertheless, the downregulation of these genes was significant only in response to As(III), with the exception for the *glk* and *pgi* genes, which were also

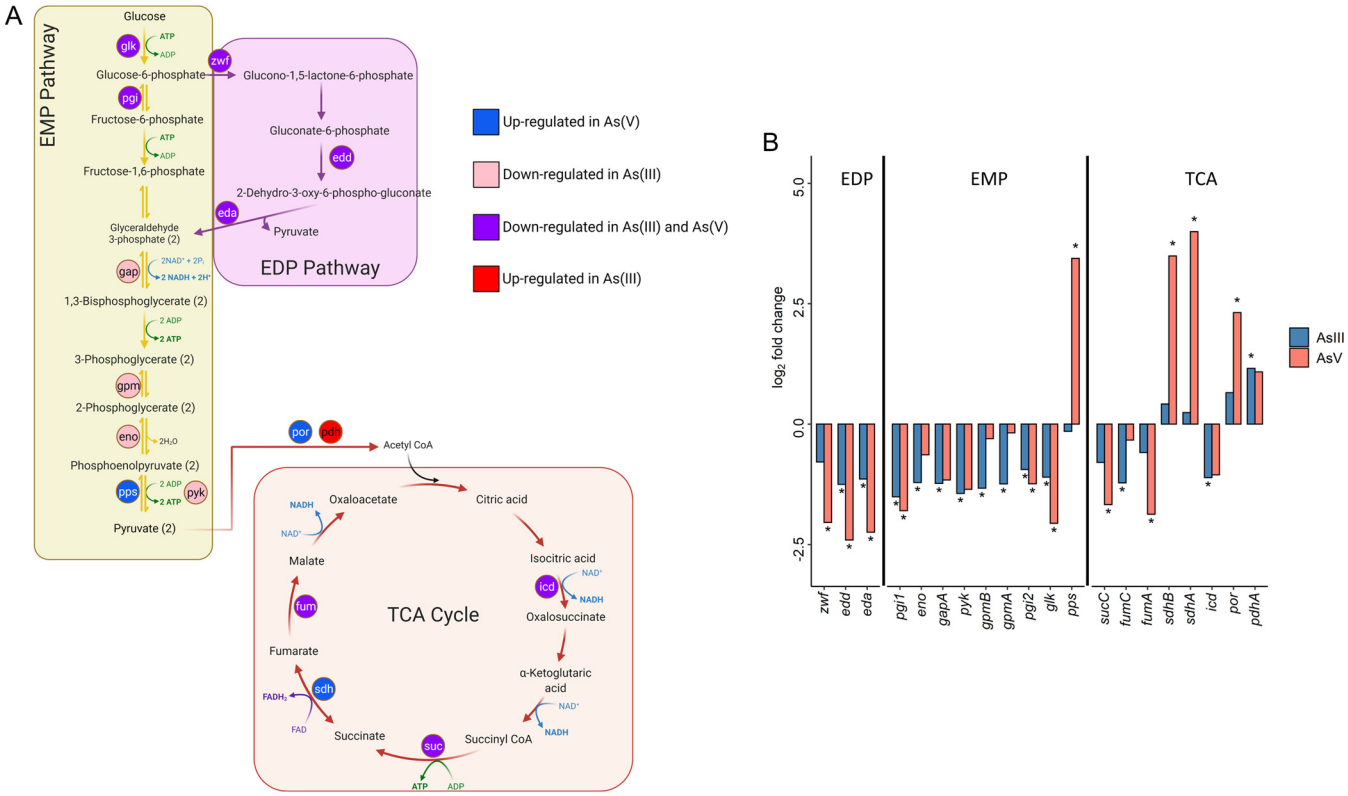

FIG 5 Differentially expressed genes (DEGs) involved in central carbon metabolism in *R. aetherivorans* BCP1 exposed to arsenic. (A) Schematic representation of the Entner-Doudoroff pathway (EDP) (purple), Embden-Meyerhof-Parnas (EMP) pathway (yellow), and tricarboxylic acid (TCA) cycle (red). The enzymes are indicated in colors that indicate their differential expression (up- or downregulation at the transcriptional level) in the presence of 5 As(III) and/or 30 mM As(V) compared to the control condition (i.e., absence of metal). (B) Asterisks indicate statistically significant differences (FDR $<$ 0.01) in the gene expression levels detected in As(III)- and As(V)-exposed BCP1 cells compared to the control condition (i.e., absence of metal). In the x axis the gene names are indicated without considering the relative position on the genome. Raw data used for the bar plot are reported in Table S5. KEGG Orthology (KO) annotation of the genes in panel A is reported in Table S1.

strongly inhibited by As(V). These data indicate that the enzymes involved in the EMP reactions releasing high-energy molecules, i.e., ATP and NADH, are downregulated in response to both the arsenic oxyanions.

Some differences in expression changes induced by As(III) and As(V) were observed for the genes encoding enzymes of the tricarboxylic acid (TCA) cycle. While both the arsenic species downregulated the genes *suc*, *fum*, and *icd*, As(V) significantly induced the expression of *por* (pyruvate oxidoreductase) and *sdh* (succinate dehydrogenase), the latter being involved in the formation of reducing power ($FADH_2$) for oxidative phosphorylation (Fig. 5; Table S5).

Notably different effects of As(III) and As(V) were detected for genes involved in cell growth and division. All BCP1 genes responsible for cell division, including the cell wall cluster (*dcw*), were upregulated by As(V), although only *sepF* was strongly expressed compared to the control condition. Conversely, all these genes were significantly downregulated in response to As(III) (Table 3; Fig. S1B).

(iv) Fatty acid metabolism. The expression of several BCP1 genes involved in the metabolism of the fatty acids was also altered in response to both the arsenic species under analysis. However, whereas the effect of As(III) was mostly downregulation, As(V) action resulted in the upregulation of these genes. (Fig. 6; Table S6). Within this metabolism, As(III)-exposed cells upregulated a few genes that are involved in beta-oxidation, while As(V) up-regulated several genes involved in both fatty acid degradation and triacylglycerol (TAG) biosynthesis. Regarding fatty acid degradation, As(V) induced the overexpression of a series of genes involved in the beta-oxidation cycle which encode long-chain fatty acid coenzyme A (CoA) ligases, acyl-CoA dehydrogenases, a 3-hydroxyacyl-CoA dehydrogenase, and an

TABLE 3 Differentially expressed genes involved in cell division and cell wall synthesis in BCP1 cells exposed to As(III) and As(V)

		As(III)		As(V)	
Locus tag	Gene product	Log_2 fold change[a]	FDR	Log_2 fold change[a]	FDR
RS12520	Cell division protein SepF	−1.60	1.30E−04	1.96	9.28E−03
RS12525	YggS family pyridoxal phosphate-dependent enzyme	−1.13	7.01E−03	1.36	7.06E−02
RS12535	Cell division protein FtsZ	−1.26	1.63E−04	0.95	0.25
RS12545	UDP-*N*-acetylmuramate–L-alanine ligase	−0.98	9.14E−03	0.58	0.55
RS12550	Undecaprenyldiphospho-muramoylpentapeptide *β*-*N*-acetylglucosaminyltransferase	−1.14	5.93E−04	0.64	0.47
RS12555	Putative lipid II flippase FtsW	−1.10	1.36E−03	1.26	0.12
RS12585	16S rRNA (cytosine(1402)-*N*(4))-methyltransferase RsmH	−1.22	2.16E−03	0.87	0.31
RS12590	Division/cell wall cluster transcriptional repressor MraZ	−1.40	2.71E−04	1.00	0.27

[a]Relative to the control.

acetyl-CoA acetyltransferase; these enzymes provide As(V)-exposed BCP1 cells with acetyl-CoA and other metabolic precursors for NADH and $FADH_2$ generation through the TCA cycle and oxidative phosphorylation (OXPHOS).

With regard to fatty acid synthesis, both oxyanions downregulated genes involved in the fatty acid synthesis pathway (FASII) and elongation, including *fabF*, *fabG*, and *fabH* (Fig. 6; Table S6). Conversely, As(V) upregulated genes involved in the Kennedy pathway which are involved in TAG biosynthesis and phospholipid modulation, i.e., the genes encoding a diacylglycerol kinase (*dagK*), a 1-acyl-*sn*-glycerol-3-phosphate acyltransferase (*plsC*), and two different *O*-acyltransferases (*tgs1* and *tgs3*) in the wax ester/triacylglycerol synthase family (also named Atf). In particular, the latter enzyme catalyzes the final step of triacylglycerol biosynthesis.

(v) Oxidative phosphorylation and energetic metabolism. Both fatty acid metabolism and the TCA cycle provide the electron donors to oxidative phosphorylation (OXPHOS) through the formation of NADH and $FADH_2$. In BCP1, the gene *sdh1*, encoding the succinate dehydrogenase (complex II) of the oxidative respiratory chain, was strongly upregulated in the presence of As(V) (Fig. 7B; also, see Table S7). Notably, several additional gene products were found to be significantly overexpressed in response to As(V), namely, (i) *nuo* and *ctaD*, coding for NDH-1 (NADH-quinone oxidoreductase) and subunit I of the cytochrome aa_3 oxidase, respectively; (ii) *codh*, encoding carbon monoxide dehydrogenase; (iii) *hyd* genes, encoding the [NiFe] hydrogenase complex, which catalyzes the reversible

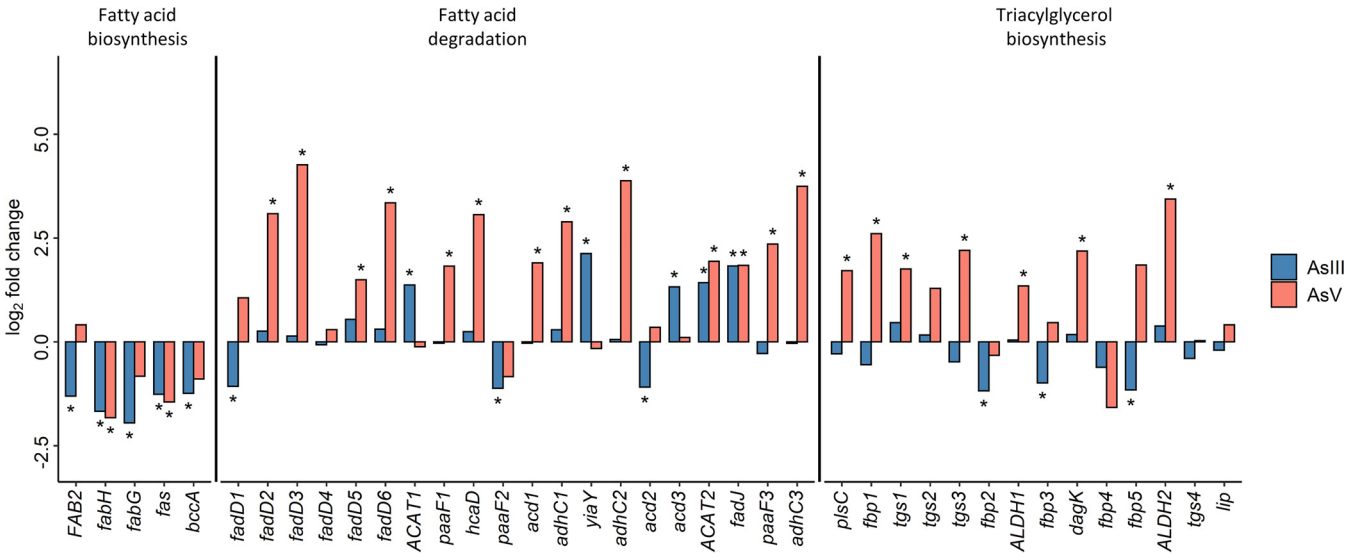

FIG 6 Fatty acid metabolism-related differentially expressed genes (DEGs) induced in *R. aetherivorans* BCP1 exposed to arsenic. Asterisks indicate statistically significant differences (FDR < 0.01) in the gene expression levels detected in As(III)- and As(V)-exposed BCP1 cells compared to the control condition (i.e., absence of metal). Genes were assigned to fatty acid degradation/biosynthesis pathways and the triacylglycerol (TAG) pathway according to the KEGG Orthology (KO) annotation terms. Raw data are reported in Table S6. KEGG Orthology (KO) annotation of the genes is reported in Table S1. In the x axis the gene names are indicated without considering the relative position on the genome.

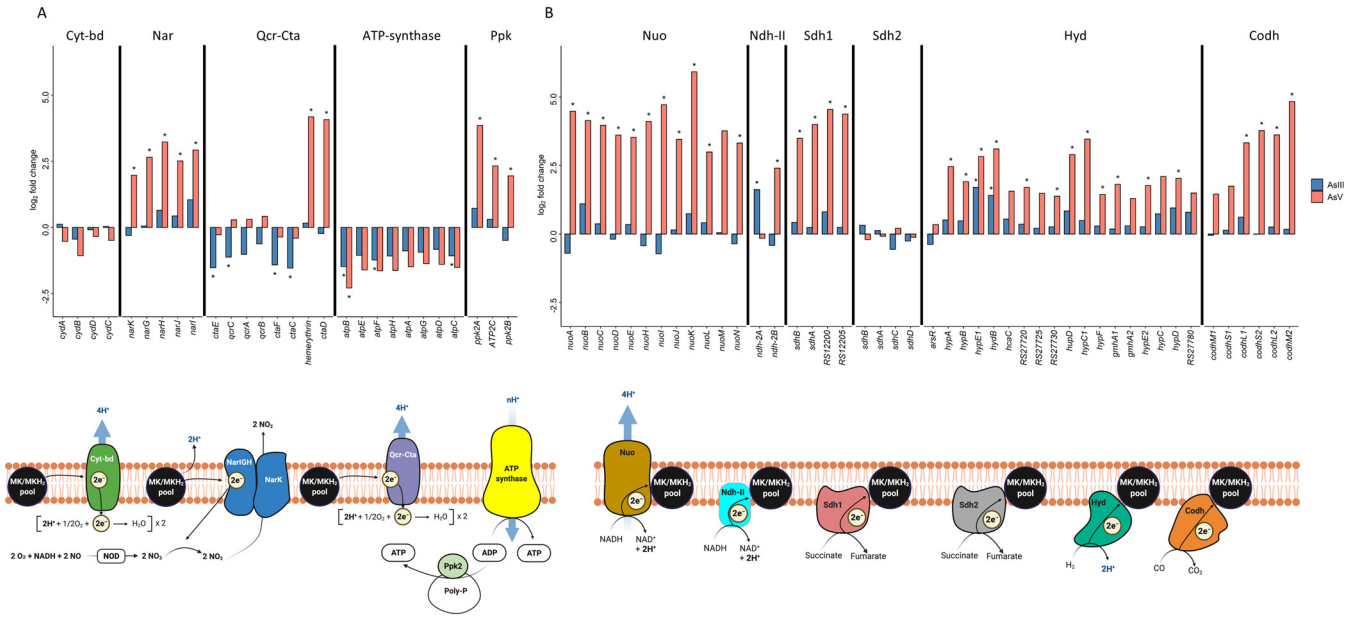

FIG 7 Differentially expressed genes (DEGs) involved in oxidative phosphorylation and polyphosphate kinase activity in *R. aetherivorans* BCP1 exposed to arsenic. The schematic representation and differential gene expression of the genes involved in the upper (A) and lower (B) pathways of the oxidative phosphorylation in BCP1. The organization of complex within OXPHOS is displayed below each bar plot. Hypothetical proteins are labeled with the RefSeq locus tag ("RS" followed by a number). Asterisks indicate statistically significant differences (FDR < 0.01) in the gene expression levels detected in As(III)- and As(V)-exposed BCP1 cells compared to the control condition (i.e., absence of metal). In the x axis (in A and B) the gene names are indicated without considering the relative position on the genome. Raw data are reported in Table S7. KEGG Orthology (KO) annotation of the genes in panel A are reported in Table S1.

oxidation of molecular hydrogen ($H_2 \leftrightarrow 2H^+ + 2e^-$); and (iv) *nar* genes, encoding the respiratory nitrate reductase (Fig. 7; Table S7).

Further, the two *ppk2* genes, encoding the polyphosphate kinases of class 2, were also significantly overexpressed in response to As(V); these enzymes catalyze the phosphorylation of AMP and/or ADP to ATP, using polyphosphate as a P_i source. However, the ATP synthase genes were downregulated in response to both arsenic species [As(III) and As(V)]. As (III) also significantly dowregulated the proton-pumping cytochrome *bcc-aa*$_3$ supercomplex (quinol/*bcc-aa*$_3$ oxidoreductase).

(vi) Secondary-metabolite production. antiSMASH (Antibiotics and Secondary Metabolite Analysis Shell) is software capable of identifying genes involved in the synthesis of secondary metabolite compounds. This bioinformatic analysis identified 19 potential biosynthetic gene clusters in *R. aetherivorans* BCP1 genome (Table S8). Among these, As(V) significantly upregulated some genes involved in the biosynthesis of the mycofactocin, which is a redox cofactor resembling pyrroloquinoline quinone (PQQ) cofactor and bacteriocin (25) (Fig. 4), and differentially expressed genes in biosynthetic gene clusters (BGC) predicted to be involved in the synthesis of heterobactin A-like (*htb*) (Fig. 8A) and coelichelin-like (*cch*) siderophores (Table S9). While the coelichelin gene cluster predicted via antiSMASH included several genes differentially expressed in response to As(III) and As(V), the well-known biosynthetic genes *cchCDE* (first characterized in *Streptomyces coelicolor*) were not differentially regulated in response to the two arsenic species (26) (Table S9). On the other hand, the heterobactin biosynthetic genes *htbBEAC*, *htbDI* and the nonribosomal peptide synthetase (NRPS)-coding gene were downregulated in response to As(III) and As(V) (Fig. 8A). Compared to *Rhodococcus erythropolis* strains PR4 and S43, where the heterobactin was previously defined as an As(III)-chelating siderophore, the heterobactin A-like gene cluster *htb* in BCP1 presents two major differences: (i) the *htbHJK* genes, which are involved in the uptake of *htb*, are missing and (ii) two copies of the NRPS gene are present in the BCP1 genome (Fig. 8B). These differences might reflect distinct metal specificity and/or binding affinity.

DISCUSSION

In this work, we studied the transcriptional response of *Rhodococcus aetherivorans*

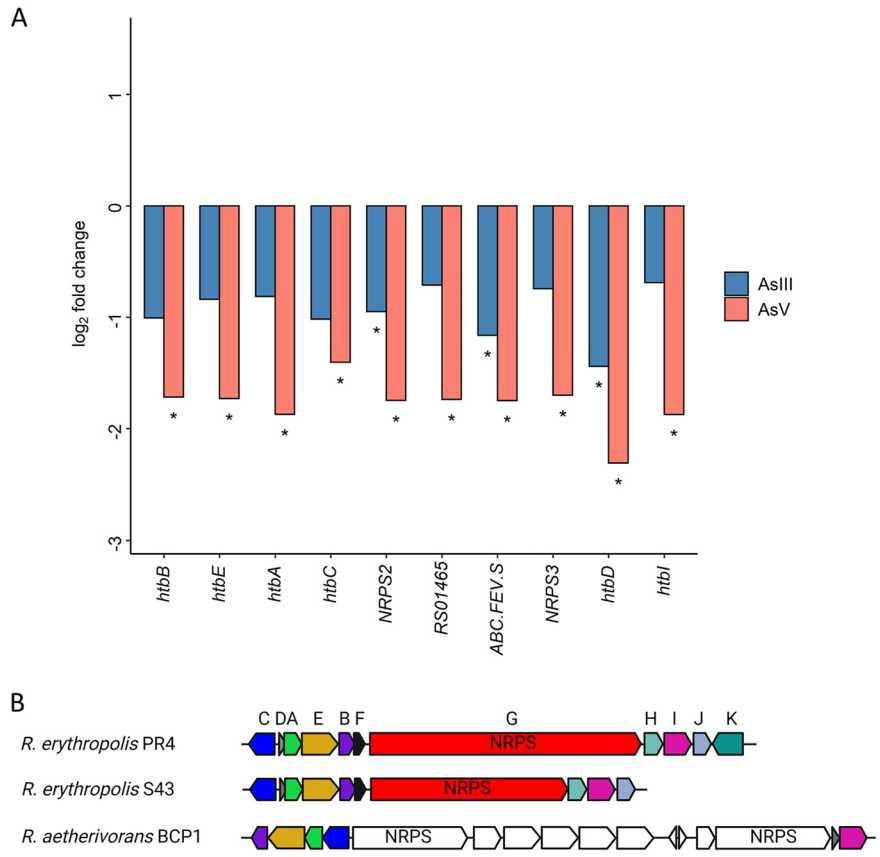

FIG 8 Differentially expressed genes (DEGs) involved in heterobactin A-like metallophore biosynthesis in *R. aetherivorans* BCP1 and comparison with other *Rhodococcus* strains. (A) Differential expression of the *htb* genes that were predicted by antiSMASH analysis to be involved in heterobactin-like metallophore biosynthesis. Asterisks indicate statistically significant differences (FDR $<$ 0.01) in the gene expression levels detected in As(III)- and As(V)-exposed BCP1 cells compared to the control condition (i.e., absence of metal). (B) Comparative analysis of the *htb* gene cluster in *R. aetherivorans* BCP1, *R. erythropolis* PR4, and *R. erythropolis* S43. Orthologous genes shared between BCP1, PR4, and S43 are shown with the same color. Raw data used for the bar plot are reported in Table S9.

BCP1 induced by the two main inorganic arsenic oxyanions supplied at concentrations that were previously observed to induce opposite growth phenotype (14). Specifically, while 5 mM As(III) caused cell growth delay because of its toxicity, the exposure of BCP1 cells to 30 mM As(V) did not negatively influence their growth performance but actually seemed to temporarily improve the growth rate. Following this previous observation, this study shows that indeed the patterns of glucose consumption and intracellular ATP level are similar between the control and As(V)-exposed cells, while they are greatly affected by As(III). In association with this, we also observed a distinct global transcriptional response induced in BCP1 by the two arsenic species. In fact, only around 7% of the DEGs were shared between the two transcriptomic patterns, indicating that each arsenic species activates distinct response patterns in BCP1. The main differences were revealed at the level of expression of the genes, which are involved in several cellular processes/metabolisms (discussed below), including arsenic resistance mechanisms, stress response, redox homeostasis, central metabolism, and bioenergetics.

Arsenic resistance mechanisms in BCP1. A previous study proposed that the main mechanism of arsenic detoxification in BCP1 cells involves the reduction of As(V) to As(III) through the activity of enzymes encoded by *ars* genes (14). Accordingly, in this work, we observed the upregulation of the *ars* genes in response to both As(III) and As(V), although only with As(III) the expression was significantly different from that of the control. These data confirmed previous results (14) that documented the transcriptional induction of *ars* gene cluster by 30 mM As(V). The higher induction of *ars* genes by As(III) than As(V) could

be explained based on previous results described with *Corynebacterium glutamicum* (27), in which As(III) was found to be the actual inducer of *ars* gene expression, because of its inactivation of the transcriptional repressor of *ars* genes, ArsR. Conversely, *arsI*, which is located outside the *ars* gene cluster and encodes the C-As lyase, was significantly expressed in the presence of both As(III) and As(V). The activity of ArsI has been previously associated with the detoxification of methylarsenite and generally in the degradation of organo-arsenicals (28). We hypothesize that the upregulation of the *arsI* gene by both inorganic As species could be due to the intracellular formation of organo-arsenical species during the arsenic detoxification process. Although no genes could be directly associated with arsenic methylation in BCP1 (no *arsM* gene is present in the BCP1 genome), other complex organo-arsenicals (i.e., arseno-sugars, arseno-lipids, and arseno-betaine) might be competitively inserted into various synthetic pathways or via still-unknown enzymatic reactions (29). In general, *ars* genes commonly related to the resistance to organic arsenicals (e.g., *arsP*, *arsM*, *arsJ*, and *arsH*) are rare not only in *Rhodococcus* strains but also in *Actinobacteria*. Conversely, *ars* genes involved in the detoxification of inorganic arsenic species (e.g., *arsC*, *arsA*, *acr3*, *arsT*, *arsX*, *arsD*, and *arsR*) are evenly distributed, indicating that the mechanisms of resistance to As(III) and As(V) are conserved in this phylum (14).

In addition to the phenotypic difference between 5 mM As(III) and 30 mM As(V), previous work (14) described very different MICs of the two arsenic species for BCP1 cells [$>$240 mM As (V) and $>$8 mM As(III)]. This type of result might be explained by assuming that the reduction of As(V) to As(III) is not the only arsenic detoxification process occurring in BCP1 cells and that additional resistance/response mechanisms should exist to cope with the As(III) that is intracellularly produced through As(V) reduction. Intracellular or extracellular binding of the newly generated As(III) could be involved in lowering its toxicity by sequestering it (13). In *Actinobacteria*, the capacity to chelate As(III), mediated by siderophores, was observed in *Kocuria rosea*, *Arthrobacter oxydans*, and *R. erythropolis* isolates (30). Further studies demonstrated that in *R. erythropolis* strain S43, As(III) binding was performed by heterobactin, a siderophore structurally and chemically characterized in *R. erythropolis* PR4 (31–33). A BGC coding for enzymes involved in the synthesis of a heterobactin A-like siderophore is also present in BCP1, although its gene content is very different from that described in *R. erythropolis* PR4 and S43 (Fig. 8B). Furthermore, these genes are downregulated in response to As(III) and As(V) (Fig. 8A). While the genetic differences could reflect distinct binding specificity for metals, the transcriptional downregulation could limit the cellular uptake of arsenic.

Different enzymes are involved in BCP1 oxidative stress responses induced by As(III) and As(V). Arsenic is known to be a highly toxic element that induces the production of a variety of ROS (e.g., superoxide, peroxyl radicals, nitric oxide, and hydrogen peroxide) (34). Cells usually counteract the oxidant effects of arsenic compounds by the activity of catalase, superoxide dismutase, and nitric oxide dioxygenases (35). The transcriptomic profile of BCP1 reported in this work showed that significant upregulation of catalases and nitric oxide dioxygenases was induced in response to the exposure to both arsenic species, whereas neither of them induced superoxide dismutase. The induction of an antioxidant machinery was functionally supported by the results we obtained on the capacity of BCP1 to degrade high levels of H_2O_2 when treated with As(III) or As(V); specifically, As(III)-exposed cells were the most efficient in detoxification. This difference might be associated with the induction of different *kat* and *nod* genes by each of the two arsenic species and/or possibly with the diversity in the expression levels. Indeed, catalases belonging to distinct classes (e.g., KatE and KatG) have been shown to have different ROS-scavenging activities (36). The organization of these genes in operon structure with specific regulatory genes and/or other stress-related genes suggested that one of the reasons for the specific upregulation was the distinct regulatory circuits and stress-response mechanisms induced by the two arsenic compounds. Based on the gene proximity and transcriptional induction, the activity of Fur regulators related to iron abundance might regulate the expression of the As(III)-responsive KatE and the As(V)-responsive KatG (37). The As(III)-responsive KatE could be also associated with the activity of Dps, which protects DNA from oxidative damages and was previously found to be induced in *Rhodococcus jostii* RHA1 under desiccation stress (38). The *katE* response to As(V) seems to be associated with the intracellular level of c-di-GMP through the regulatory

activity of a protein containing a GAF domain (AcoR/FisR). Accordingly, previous studies described the role of this secondary messenger in the modulation of the activity of catalases and other ROS/RNS-scavenging enzymes involved in the bacterial response to abiotic stresses (39–41).

In terms of protection mechanisms against oxidative damage, the production of the enzymes (Ahp, Nem, Msr, and rhodanese; see "Stress response") involved in repairing oxidative injuries of cellular targets sensitive to peroxidation (i.e., lipids, DNA, and methionine and cysteine residues in proteins), suggests that As(III) acts as a strong oxidant in BCP1 cells (42). Additionally, we found that As(III) downregulated the genes involved in BCP1 cell division and peptidoglycan (diaminopimelic acid) synthesis. This suggests that a typical survival strategy was activated during the bacterial response to DNA damage, and cell division was halted until favorable growth conditions occurred (43). The involvement of different antioxidant defenses against very strong oxidants and their efficiency in pathogenic and nonpathogenic *Mycobacterium* strains were previously reported (44). Different oxidants and different levels of oxidative stress induced diverse individual antioxidant defense enzymes or their collective action (44). According to the levels of induced enzymes and proteins that cope with the As stress, As(V) activated more proteins, which were involved in the recovery and degradation (via pupylation) of mis- or unfolded proteins than As(III)-activated proteins. This suggests that the exposure of BCP1 cells to As(V) causes a strong accumulation of unfolded proteins and protein aggregates which require the activity of chaperones and proteasomal proteins. Previous studies described chaperones and proteasomal proteins as being intimately interconnected with cell viability in *Actinobacteria* strains (45–47), and this could support our findings on the absence of a BCP1 cell growth defect in the presence of As(V). Indeed, these proteins might not only be part of the stress response apparatus of BCP1 but also actively contribute to its growth sustainment in the presence of this arsenic form. In agreement with the apparently stimulated growth, genes associated with cell duplication/growth were upregulated in As(V)-exposed BCP1 cells.

Cofactors and antioxidants that contribute to redox balance in BCP1 response to As(III) and As(V). The exposure of BCP1 cells to the two arsenic species induced the expression of genes encoding different redox homeostasis systems, i.e., mycothiol with As(III) and ergothioneine with As(V). As(V) also upregulated the *mft* genes, which are involved in the biosynthesis of the poorly characterized redox-cofactor mycofactocin (MFT) (48). These results suggest the existence of distinct mechanisms of intracellular redox homeostasis in BCP1 cells exposed to the two arsenic species. In particular, BCP1 cells exposed to As(III) induced the overexpression of genes involved in mycothiol (MSH) biosynthesis and their regulation (*sigH* and *anti-sigH*). MSH is a functional analog of glutathione (GSH) that was found in different actinomycetes, such as *Rhodococcus*, *Mycobacterium*, and *Streptomyces* (49). In *Rhodococcus jostii* RHA1 as well as in other model actinomycetes (*Streptomyces coelicolor*, *Corynebacterium glutamicum*, and *Mycobacterium smegmatis*), the disruption of genes involved in MSH synthesis affected cellular phenotypes, including the susceptibility to antimicrobials (50). Conversely, in the presence of As(V), BCP1 cells overexpressed the genes *egtABCD*, which drive the biosynthesis of ergothioneine (EGT). Mycothiol and ergothioneine, whose biosynthesis was induced by As(III) and As(V), respectively, have recently been described to protect *Mycobacterium tuberculosis* from oxidative stress and support detoxification pathways (20). Unlike MSH, EGT is synthesized by a variety of microbes, especially fungi and actinobacteria (51). The amount of EGT present in actinomycetes is 10-fold lower than that of MSH, and its exact function in bacterial cells is still unknown (52). Notably, a recent study on *M. tuberculosis* reported that EGT modulates drug sensitivity and that EGT and MSH are both essential for redox and bioenergetic homeostasis in actinomycetes (20). In line with this, we have evidence that BCP1 cells control the intracellular level of both EGT and MSH in response to arsenic, although each of these two redox buffers seems to be specifically involved in the intracellular redox potential balance in the presence of either As(III) or As(V). The specificity of each of the two redox buffers could be associated with the different reduction potential ($E^{0\prime}$) (53), allowing BCP1 to specifically respond to a different spectrum and levels of reactive species that are produced

in the presence of As(III) or As(V) (54). In addition to EGT, As(V) induced the overexpression of genes involved in MFT synthesis. MFT's role in *Mycobacterium* as a fitness factor during infection and as a cofactor involved in the electron transport chain (25, 48) suggests its positive role during BCP1 growth in the presence of As(V).

Production of acetyl-CoA in As(V)-exposed cells. In BCP1 exposed to As(V), the TCA precursor acetyl-CoA can be generated through metabolic routes that are alternatives to glycolysis. Indeed, glucose consumption does not seem to be affected by this arsenic species, although glycolytic genes are downregulated. This might be due to the involvement of alternative pathways in glucose metabolism (e.g., the pentose phosphate pathway) or to a change in kinetics also related to the omission of the reaction catalyzed by the phosphoglycerate kinase. This bypass is caused by the formation of an unstable intermediate known as 1-arseno-3-phosphoglycerate that spontaneously hydrolyzes to 3-phosphoglycerate (55). Conversely, in As(III)-exposed cells, the downregulation of glycolytic genes is accompanied by a negative impact on glucose consumption. This is in line with the well-known inhibition of numerous physiologically relevant enzymes and a more general negative effect on cellular growth and metabolism (56). Thus, based on the transcriptomic pattern observed in this work, other genes could be involved in the acetyl-CoA production in BCP1 cells exposed to As(V). This can proceed through (i) the activity of the pyruvate-ferredoxin/flavodoxin oxidoreductase (Por), (ii) the biosynthesis of ergothioneine, and (iii) fatty acid biodegradation. The possible contribution of Por to acetyl-CoA synthesis through pyruvate decarboxylation was suggested by a recent work reporting Por activity and NADPH generation in aerobic bacteria under oxidative stress (57, 58). Furthermore, the biosynthesis of EGT was also recently described as a source of acetyl-CoA (20). Indeed, the biosynthesis of EGT releases pyruvate, which can be converted to acetyl-CoA, connecting the generation of this redox buffer with glycolysis and the TCA cycle (20). Accordingly, EGT was previously suggested to contribute not only to the redox potential maintenance but also to bioenergetic homeostasis. Furthermore, the production of EGT was also suggested to be associated with the cell proliferation of eukaryotic cells (59). These indications suggest that the upregulation of genes involved in ergothioneine synthesis in the presence of As(V) might create a connection between stress response, central metabolism, and possible anabolic pathways supporting cell synthesis and duplication in BCP1 cells.

DEG analysis also suggested that the fatty acid degradation pathway may provide BCP1 cells with acetyl-CoA and reducing power in the presence of As(V). Specifically, a series of homologous genes involved in beta-oxidation are induced in response to As(V). The presence and induction of homologous genes involved in fatty acid metabolism are typical of *Rhodococcus* strains that possess multiple copies of genes involved in fatty acid functionalization being indicative of the wide catabolic and anabolic activities in relation with fatty acids (60). Furthermore, As(V) induces the transcription of genes in the Kennedy pathway, including that for diacylglycerol *O*-acyltransferase/wax synthase, which catalyzes the final step of triacylglycerol (TAG) biosynthesis. Kennedy pathway enzymes can be involved in both TAG biosynthesis and phospholipid modulation, suggesting an active rearrangement and modulation of lipid storage and membrane composition in response to As(V). The role of TAG accumulation in As(V)-exposed BCP1 cells might be similar to its role in *Mycobacterium* strains, in which the production of TAGs was suggested to significantly contribute to persistence under different stress conditions, i.e., low oxygen, high CO_2, low nutrients, and acidic pH (61). Specifically, mycobacterial strains showed increased phenotypic drug tolerance in association with TAG accumulation. While in bacteria there is no association between arsenic exposure and TAG accumulation, an increase in lipid accumulation was found to be induced by arsenic exposure in microalgae (62), although the mechanisms are still unknown.

On the other hand, the upregulation of a few genes involved in fatty acid degradation and the downregulation of genes involved in fatty acids and TAG biosynthesis in the presence of As(III) suggest that the exposure of cells to this oxyanion activates mechanisms of survival and oxidative stress response that funnel the metabolism away from anabolic processes, including those associated with fatty acids.

Rearrangement of central and OXPHOS metabolism induced by arsenic anions. According to genome annotation, the respiratory redox chain of *R. aetherivorans* BCP1

shares several features of the saprophytic soil actinobacterium *M. smegmatis* (Fig. 7). The latter species possesses a branched respiratory chain leading to one of two terminal oxidases, the cytochrome *bcc-aa*$_3$ supercomplex or the cytochrome *bd* oxidase (63). The proton-pumping cytochrome *bcc-aa*$_3$ supercomplex is the more efficient of these two complexes, and it is mainly used during aerobic growth of *M. smegmatis* (63, 64). On the other hand, the non-proton-pumping *bd* complex is predicted to have a higher affinity for O_2 and is important during nonreplicative persistence, a property also found in the pathogenic species *M. tuberculosis* and *M. leprae* (65). In actively growing *M. smegmatis*, electrons entering the respiratory chain are derived from heterotrophic substrates and are donated to the respiratory chain by NADH largely via the non-proton-pumping type II NADH dehydrogenase (NDH-2) and succinate via the succinate dehydrogenase SDH1 (63). Although *M. smegmatis* is a strict heterotroph, it is able to aerobically respire using CO at atmospheric concentrations during carbon-limited persistence by means of a carbon monoxide dehydrogenase (66). It has likewise been predicted that two membrane-associated hydrogenases, Huc and Hhy, support survival under continued stress by providing electrons derived from H_2 to the respiratory chain (67), although it remains to be definitively demonstrated that H_2 serves as a respiratory electron donor in this organism. Notably, most of the genes coding for the OXPHOS respiratory redox complexes in BCP1 cells showed both composition and arrangement similar to those of *M. smegmatis* and *M. tuberculosis* (this work). Indeed, the present transcriptomic analysis confirms and extends early biochemical observations in a few actinobacteria (68) and more specifically in *Rhodococcus rhodochrous* (69) indicating the presence in these species of branched respiratory chains composed of a cytochrome *bcc-aa*$_3$-type complex and a *bd*-type oxidase. We report the presence in BCP1 of a proton-pumping NDH-1 (*nuo* genes), a non-proton-pumping NDH-2 (*ndh*; gene ID, Rv1854c) having 67% similarity with the NDH-2 counterpart in *M. smegmatis*, and a second non-proton-pumping NDH-2-like protein (*ndhA*; gene ID, Rv0392c) which has only 43 to 44% sequence similarity to the other NDH-2 (data not shown). The lower part of the electron transport chain also includes two succinate dehydrogenases (SDH1 and SDH2), a menaquinone pool ($E_h = -74$ mV) composed mainly of hydrogenated menaquinone-8 [MK-8(H_2)] (70), a carbon monoxide dehydrogenase (CODH), and a Ni-Fe hydrogenase (HYD) complex, the latter enzyme catalyzing the oxidation of molecular hydrogen.

In BCP1 cells exposed to As(III), a large set of genes involved in the central and energetic metabolism as well as cell division/growth, including the vegetative sigma factor A gene, which regulates the basal cellular functions, were downregulated. This suggests that in the presence of arsenite, the transcriptional cell response is tuned to survival strategies that limit cell growth, possibly due to the strong oxidant activity of As(III). Alternatively, As(V) differentially upregulates a series of genes involved in the TCA cycle and oxidative phosphorylation, a response that resembles previously reported work in a few species of the genus *Mycobacterium* (63, 65). In particular, similarly to mycobacterial cells under a reduced O_2 supply, the exposure to As(V) induced in BCP1 the overexpression of genes encoding the phosphoenolpyruvate synthase (Pps) and the pyruvate-ferredoxin/flavodoxin oxidoreductase (Por), while the energetic metabolism showed some similarities with that previously described for *Mycobacterium* under energy-limiting conditions (63, 65). This includes the downregulation of the gene cluster for the F_1F_o-ATP synthase and the upregulation of the *sdh1* (succinate dehydrogenase [SDH1]), of the two gene clusters encoding Ni-Fe hydrogenases, of the *nuo* gene cluster, encoding the NADH-menaquinone oxidoreductase (NDH-1), and of the *codh* genes, coding for carbon monoxide dehydrogenase (CODH) (63, 71). Other similarities include the upregulation of the soluble di-iron monooxygenases and a series of dehydrogenase activities. However, in contrast to *Mycobacterium* under energy-limited conditions, genes encoding the heme/redox complexes MK–*bcc-aa*$_3$ supercomplex, *bd*-menaquinol oxidase, and the second succinate dehydrogenase (SDH2), suggested to function as a fumarate reductase in *M. smegmatis*, were downregulated upon As(V) exposure. These findings suggest that, on the one hand, some transcriptional rearrangements are common among different type of stresses and *Actinobacteria* strains and that, on the other, the transcriptional response to As(V) presents uniqueness and specificity.

In the presence of As(V), the nitrate reductase Nar was significantly upregulated in BCP1 cells. The Nar enzymatic system of BCP1 is expected to transfer $2e^-$ from the

menaquinol (MKH_2) pool to NO_3 (nitrate) to reduce it to NO_2 (nitrite). Since under the conditions used for the growth of BCP1, NH_4^+ (ammonium) was the only source of nitrogen, it could be hypothesized that nitrate is the by-product of NO (nitric oxide) reduction through the NADH-dependent nitric oxide dioxygenase (NOD, RS18025) activity. As previously reported for *Enterobacterium* strain LSJC7 (72), a consistent intracellular production of toxic NO was detected in As(V) (32 mM)-stressed cells. Therefore, in this scenario, the observed upregulation of the *nar* operon would be linked to NO detoxification, as NAR activity was also associated with NO stress resistance in *Mycobacterium* (63, 73) along with bacterial resistance to other metalloid oxyanions, such as tellurite and selenate (74).

The nonheme, di-iron, O_2-binding hemerythrin-like proteins are present in all domains of life (75, 76), and experimental evidence suggests that they can function as oxygen sensors and reserves, as well as mediating the delivery and transport of this diatomic gas (76). In this respect, hydrogen peroxide (H_2O_2) is one of a variety of reactive oxygen species (ROS) produced by aerobic organisms, and it has been reported that a *Mycobacterium smegmatis* hemerythrin-like protein, MSMEG_2415, is an H_2O_2-modulated repressor of the SigF-mediated response to H_2O_2. Notably, in BCP1, As(V) upregulates a gene cluster that codes for a hemerythrin-like protein (N505_RS09685) and for catalytic subunit I (CtaD; N505_RS09690) of the cytochrome aa_3 oxidase (COX).

These data, therefore, seems to indicate that BCP1 can regulate single components of the respiratory complexes in response to specific stressors. Furthermore, As(V) does not differentially regulate the genes coding the upper part of the respiratory chain components, i.e., cytochrome *bd* oxidase and the cytochrome *bcc-aa*$_3$ supercomplex, but only downregulates (although not significantly) the transcription of F_1F_o-ATP synthase genes. This suggests that As(V) induces the respiratory chain activity not to generate proton motive force (PMF) for the synthesis of ATP but to oxidize NADH with the upregulation of NDH-1 (Nuo) (proton-translocating complex) and NDH-2 (non-proton-translocating complex). This could indicate, as already suggested for *M. smegmatis* and *M. tuberculosis* (63), that *R. aetherivorans* BCP1 has no alternative mechanisms for recycling NADH during aerobic growth under As(V) stress conditions, necessitating the maintenance of the membrane potential both for the vital functions of the cell via NDH-1 and for the disposal of any excess of NADH via NDH-2. On the other hand, the parallel overexpression of the *ppk2* genes suggests a possible contribution of the polyphosphate kinase of family 2 to ATP generation by using polyphosphate granules (77). Indeed, polyphosphates were previously associated with mechanisms of bacterial resistance/tolerance to toxic organic compounds and metals (6, 78, 79).

Taken together, the present transcriptomic analysis indicates that the response to 5 mM As(III) of *R. aetherivorans* BCP1 cells is mostly associated with processes of cell survival and damage recovery from strong oxidative stress. Conversely, 30 mM As(V) activates the overexpression of stress response mechanisms alternative to those generated by As(III) and induces the rearrangement of catabolic and biosynthetic pathways that seem to be associated with energy transduction mechanisms and boosting of the growth rate. Our results provide an overview of the peculiar response of a *Rhodococcus* strain to arsenic oxyanions, laying the groundwork for future studies on the stress response and resistance/tolerance mechanisms in this genus.

MATERIALS AND METHODS

Bacterial strains and growth conditions. *Rhodococcus aetherivorans* BCP1 (DSM 44980) was routinely grown on LB and M9 medium for streaking and preinoculum from the cell stock and for cell culture preparation for RNA extraction, respectively. In particular, for RNA extraction and ATP quantification, BCP1 cultures were grown on M9 minimal medium amended with 0.2% (wt/vol) glucose as the sole carbon source. Once the cell growth reached the mid-exponential phase (optical density at 600 nm [OD_{600}] = 0.4 to 0.5), either 30 mM As(V) or 5 mM arsenite As(III) was added to the BCP1 cell cultures. These concentrations were selected based on the results recently described by the Cappelletti group (14). After the addition of the metal, BCP1 cells were further incubated for 18 h in a rotary shaker at 150 rpm. Control tests were conducted without adding arsenic. Each condition was tested in triplicate.

Total ATP quantification, glucose consumption, and ROS detoxification assays. The quantification of the total ATP and glucose consumption was performed on BCP1 cells grown up to an OD_{600} of 0.5 and exposed to 30 mM As(V), 5 mM As(III), or no metal (control condition) for 0, 2, 8, and 18 h. The measurement of H_2O_2 degradation was conducted using the same cell cultures only after 18 h of

TABLE 4 Gene targets and primer sequences used in reverse transcriptase qPCR

Gene	Locus tag	Forward primer (5′-3′)	Reverse primer (5′-3′)	Reference
sigH	N505_RS14340	TATATCAAGGCGTTCTCCGCC	CTGCTTCTTGCGGTAGGAGT	This study
narH	N505_RS08835	ATGTACAAGCGTGTCGAGGA	GATAGCACAGCGTGCACTTC	This study
cdo1	N505_RS26740	GCAGAGAACCGAAATCCACG	TCTTGCGTGACAACGCTACT	This study
mraZ	N505_RS12590	TACCCACACACCCAAGCTG	AAAGACGGAAAGGCTGTGGT	This study
ppk2	N505_RS21705	GAGCAAGATCCCCTACGAGC	GGAGTGGGTATCCAGTGCAG	This study
luxR	N505_RS28820	GCGTCGAGGTGGGCTAATAA	GACGATACTGTGACCCGGTG	This study
smoA	N505_RS28825	CTTGGTCGGATACAGTGCGTC	TACATCGGTCACAACTCAGCA	24
acr3	N505_RS21285	CGCCATGGTCATCATCTGGA	GTGGTCTGTTCGAGTCCGAG	14
fadR	N505_RS19055	CAGGGCCTGGTACGAATCAA	GATCTGGCGTCCTCGAATGA	This study

exposure. For the total ATP quantification, after harvesting 1.0 mL of each cell culture and washing the pellets twice with 0.5 mL of phosphate buffer solution (PBS), 200 μL from each suspension was transferred in a 1.5-mL tube and subjected to protein extraction by adding 40 μl of 1 N NaOH. Cell debris was separated via centrifugation, and the supernatant was collected for protein quantification. The remaining 300 μl of PBS cell suspension was mixed with 120 μl of 12% perchloric acid (PCA) by vortexing for 30 s. After this, 20 μl of a solution composed of K_2CO_3 (3 M) and Tris (2 M) was added to each cell suspension and vortexed for 5 s. The supernatant was finally collected via centrifugation at 13,000 rpm, and a fraction of it was assayed for ATP using the luciferase ATP assay kit (Sigma-Aldrich). The concentration of ATP (in nanomolar units) in the experimental samples was normalized to the total amount of protein (in micrograms).

For glucose consumption, D-glucose concentrations in bacterial supernatants (20 μL from each culture) were determined using the glucose (GO) assay kit (Sigma-Aldrich) according to the manufacturer's protocol (Sigma). ROS detoxification activity was measured by testing the H_2O_2 degradation capacity of 25 μL of diluted cell cultures (with around 1×10^5 CFU mL^{-1}) with the Amplex Red catalase assay kit (Thermo Fisher) in the presence of an initial H_2O_2 concentration of 20 μM. This assay is based on the absorption emission of resorufin, which is the oxidation product of horseradish peroxidase generated when Amplex Red reacts with H_2O_2. The absorbance measurements at 540 nm (for glucose consumption) and 570 nm (for H_2O_2 degradation), were conducted using a VICTOR^3 multilabel plate counter (PerkinElmer Life and Analytical Sciences, Zaventem, Belgium). For the Amplex Red assay, errors in the absorbance measurements due to cellular turbidity were avoided by pelleting the cells. H_2O_2 quantification in As(III)- and As(V)-exposed cells was calculated as the percentage of H_2O_2 remaining after 30 min of reaction incubation compared to the control culture. Glucose consumption after 2, 8, and 18 h was calculated in relation with the initial time of exposure and normalized to the total amount of proteins (in micrograms). Known concentrations of glucose were used to generate the standard curve and to perform the positive control.

Protein quantification was performed by using a Qubit 4.0 fluorometer (Thermo Fisher) using a Qubit protein assay kit according to the manufacturer's protocol.

RNA extraction and sequencing. Total RNA from 3 biological replicates per condition was extracted using a Quick-RNA Miniprep Plus kit (Zymo Research) according to the manufacturer's instructions and subjected to additional DNase treatment and purification by an RNA Clean & Concentrator-5 kit (Zymo Research). The quantification of total RNA was done with a DropSense 16 instrument (Trinean) and the qualification with an RNA 6000 Nano kit in an Agilent 2100 Bioanalyzer (Agilent Technologies). The rRNA depletion for the whole transcriptome cDNA library construction was performed by a Ribo-Zero rRNA removal kit (bacteria) according to manufacturer's instructions (Illumina). The rRNA-depleted total RNA quality and quantity were assessed with an Agilent RNA Pico 6000 kit and the Agilent 2100 Bioanalyzer (Agilent Technologies). Approximately 2.5 μg of RNA (RNA integrity number [RIN] $>$ 9) underwent library preparation according to the TruSeq stranded-mRNA sample preparation guide (Illumina) and sequencing using an Illumina HiSeq 1500 system using a 70-base read length (Illumina) after quality and quantity checking of the cDNA library with an Agilent high-sensitivity DNA kit and the Agilent 2100 Bioanalyzer (Agilent Technologies).

Quantification of gene expression. High-quality paired-end reads were mapped to the *R. aetherivorans* BCP1 reference genome (GCF_000470885.1) using Bowtie2 v2.2.7 (80) with the default configurations for this type of read mapping. Read Explorer v.2.2 (81) was used for gene expression quantification and differential gene expression analysis.

Differential gene expression analysis. Differential gene expression was performed using the Bioconductor package DESeq2 1.18.1 (82) with Benjamini-Hochberg correction (false discovery rate [FDR]). Genes were selected as differentially expressed on the basis of an FDR of $<$0.01. For Gene Ontology (GO) enrichment analysis, GO terms were assigned to BCP1 genes using eggNOG (83). To identify significantly enriched GO terms, TopGO was used (https://bioconductor.org/packages/release/bioc/html/topGO.html). The antiSMASH (84) web server was used to detect possible biosynthetic gene clusters among the BCP1 genes that were differentially expressed in response to arsenic.

RT-qPCR analysis. RNA samples for real-time quantitative PCR (RT-qPCR) were subjected to RNase-free DNase treatment, and 500 ng of total RNA was retrotranscribed to cDNA as described by Cappelletti et al. (24). cDNAs were used as templates to quantify the expression of 10 genes that were found to be differentially expressed by cells exposed to As(V) and As(III) (Table 4). All reactions were performed in triplicate, and the gene expression was normalized to 16S rRNA. The relative expression of each gene was then reported as the change (*n*-fold) determined from the mean normalized expression relative to the mean normalized expression of the reference gene ($2^{-\Delta\Delta CT}$).

Data availability. RNA-seq data have been deposited in the ArrayExpress database at EMBL-EBI under accession number E-MTAB-10692.

SUPPLEMENTAL MATERIAL

Supplemental material is available online only.

SUPPLEMENTAL FILE 1, PDF file, 0.2 MB.

SUPPLEMENTAL FILE 2, XLSX file, 1.5 MB.

ACKNOWLEDGMENTS

We thank master's degree students Marta Reggio and Gabriele Bivona for their support of the experimental work.

This work was financially supported by Fondazione Carisbo (Progetto UniBo/Calgary University per l'Internazionalizzazione della Genomica dei Microorganismi) and by grant 18-13254S from the Czech Science Foundation.

Conceptualization, M.C.; funding acquisition, M.C., M.P.; supervision, M.C.; writing – original draft, A.F., M.C., D.Z. (about OXPHOS), H.D. (about sigma factors); writing – review & editing, A.F., D.Z., H.D., L.I., R.J.T., D.Z., M.P., M.C.; data curation, A.F., T.B., H.D.; formal analysis, A.F., T.B.; investigation, A.F., L.I., R.R., M.C.; validation, A.F., E.D.; visualization, A.F., E.D., H.D. All the authors read and approved the last version of the manuscript.

REFERENCES

1. Coryell M, Roggenbeck BA, Walk ST. 2019. The human gut microbiome's influence on arsenic toxicity. Curr Pharmacol Rep 5:491–504. https://doi.org/10.1007/s40495-019-00206-4.
2. Shen S, Li X-F, Cullen WR, Weinfeld M, Le XC. 2013. Arsenic binding to proteins. Chem Rev 113:7769–7792. https://doi.org/10.1021/cr300015c.
3. Ben Fekih I, Zhang C, Li YP, Zhao Y, Alwathnani HA, Saquib Q, Rensing C, Cervantes C. 2018. Distribution of arsenic resistance genes in prokaryotes. Front Microbiol 9:2473. https://doi.org/10.3389/fmicb.2018.02473.
4. Garbinski LD, Rosen BP, Chen J. 2019. Pathways of arsenic uptake and efflux. Environ Int 126:585–597. https://doi.org/10.1016/j.envint.2019.02.058.
5. Rosen BP. 2002. Biochemistry of arsenic detoxification. FEBS Lett 529:86–92. https://doi.org/10.1016/s0014-5793(02)03186-1.
6. Cappelletti M, Presentato A, Piacenza E, Firrincieli A, Turner RJ, Zannoni D. 2020. Biotechnology of Rhodococcus for the production of valuable compounds. Appl Microbiol Biotechnol 104:8567–8594. https://doi.org/10.1007/s00253-020-10861-z.
7. Donini E, Firrincieli A, Cappelletti M. 2021. Systems biology and metabolic engineering of Rhodococcus for bioconversion and biosynthesis processes. Folia Microbiol (Praha) 66:701–713. https://doi.org/10.1007/s12223-021-00892-y.
8. Cappelletti M, Pinelli D, Fedi S, Zannoni D, Frascari D. 2018. Aerobic cometabolism of 1,1,2,2-tetrachloroethane by Rhodococcus aetherivorans TPA grown on propane: kinetic study and bioreactor configuration analysis. J Chem Technol Biotechnol 93:155–165. https://doi.org/10.1002/jctb.5335.
9. Cappelletti M, Fedi S, Zampolli J, Di Canito A, D'Ursi P, Orro A, Viti C, Milanesi L, Zannoni D, Di Gennaro P. 2016. Phenotype microarray analysis may unravel genetic determinants of the stress response by Rhodococcus aetherivorans BCP1 and Rhodococcus opacus R7. Res Microbiol 167:766–773. https://doi.org/10.1016/j.resmic.2016.06.008.
10. Pátek M, Grulich M, Nešvera J. 2021. Stress response in Rhodococcus strains. Biotechnol Adv 53:107698. https://doi.org/10.1016/j.biotechadv.2021.107698.
11. Alvarez HM, Silva RA, Cesari AC, Zamit AL, Peressutti SR, Reichelt R, Keller U, Malkus U, Rasch C, Maskow T, Mayer F, Steinbüchel A. 2004. Physiological and morphological responses of the soil bacterium Rhodococcus opacus strain PD630 to water stress. FEMS Microbiol Ecol 50:75–86. https://doi.org/10.1016/j.femsec.2004.06.002.
12. de Carvalho CCCR, Fischer MA, Kirsten S, Würz B, Wick LY, Heipieper HJ. 2016. Adaptive response of Rhodococcus opacus PWD4 to salt and phenolic stress on the level of mycolic acids. AMB Express 6:66. https://doi.org/10.1186/s13568-016-0241-9.
13. Presentato A, Piacenza E, Turner RJ, Zannoni D, Cappelletti M. 2020. Processing of metals and metalloids by Actinobacteria: cell resistance mechanisms and synthesis of metal(loid)-based nanostructures. Microorganisms 8:2027–2037. https://doi.org/10.3390/microorganisms8122027.
14. Firrincieli A, Presentato A, Favoino G, Marabottini R, Allevato E, Stazi SR, Scarascia Mugnozza G, Harfouche A, Petruccioli M, Turner RJ, Zannoni D, Cappelletti M. 2019. Identification of resistance genes and response to arsenic in Rhodococcus aetherivorans BCP1. Front Microbiol 10:888. https://doi.org/10.3389/fmicb.2019.00888.
15. Presentato A, Piacenza E, Anikovskiy M, Cappelletti M, Zannoni D, Turner RJ. 2018. Biosynthesis of selenium-nanoparticles and -nanorods as a product of selenite bioconversion by the aerobic bacterium Rhodococcus aetherivorans BCP1. N Biotechnol 41:1–8. https://doi.org/10.1016/j.nbt.2017.11.002.
16. Presentato A, Piacenza E, Anikovskiy M, Cappelletti M, Zannoni D, Turner RJ. 2016. Rhodococcus aetherivorans BCP1 as cell factory for the production of intracellular tellurium nanorods under aerobic conditions. Microb Cell Fact 15:1–14. https://doi.org/10.1186/s12934-016-0602-8.
17. Presentato A, Piacenza E, Darbandi A, Anikovskiy M, Cappelletti M, Zannoni D, Turner RJ. 2018. Assembly, growth and conductive properties of tellurium nanorods produced by Rhodococcus aetherivorans BCP1. Sci Rep 8:3923. https://doi.org/10.1038/s41598-018-22320-x.
18. Tucker NP, Hicks MG, Clarke TA, Crack JC, Chandra G, Le Brun NE, Dixon R, Hutchings MI. 2008. The transcriptional repressor protein NsrR senses nitric oxide directly via a [2Fe-2S] cluster. PLoS One 3:e3623. https://doi.org/10.1371/journal.pone.0003623.
19. Most P, Papenbrock J. 2015. Possible roles of plant sulfurtransferases in detoxification of cyanide, reactive oxygen species, selected heavy metals and arsenate. Molecules 20:1410–1423. https://doi.org/10.3390/molecules20011410.
20. Saini V, Cumming BM, Guidry L, Lamprecht DA, Adamson JH, Reddy VP, Chinta KC, Mazorodze JH, Glasgow JN, Richard-Greenblatt M, Gomez-Velasco A, Bach H, Av-Gay Y, Eoh H, Rhee K, Steyn AJC. 2016. Ergothioneine maintains redox and bioenergetic homeostasis essential for drug susceptibility and virulence of Mycobacterium tuberculosis. Cell Rep 14:572–585. https://doi.org/10.1016/j.celrep.2015.12.056.
21. Lupoli TJ, Fay A, Adura C, Glickman MS, Nathan CF. 2016. Reconstitution of a Mycobacterium tuberculosis proteostasis network highlights essential cofactor interactions with chaperone DnaK. Proc Natl Acad Sci U S A 113:E7947–E7956. https://doi.org/10.1073/pnas.1617644113.
22. Küberl A, Polen T, Bott M. 2016. The pupylation machinery is involved in iron homeostasis by targeting the iron storage protein ferritin. Proc Natl Acad Sci U S A 113:4806–4811. https://doi.org/10.1073/pnas.1514529113.
23. Sharp JO, Sales CM, LeBlanc JC, Liu J, Wood TK, Eltis LD, Mohn WW, Alvarez-Cohen L. 2007. An inducible propane monooxygenase is responsible for N-nitrosodimethylamine degradation by Rhodococcus sp. strain RHA1. Appl Environ Microbiol 73:6930–6938. https://doi.org/10.1128/AEM.01697-07.
24. Cappelletti M, Presentato A, Milazzo G, Turner RJ, Fedi S, Frascari D, Zannoni D. 2015. Growth of Rhodococcus sp. strain BCP1 on gaseous n-alkanes: new metabolic insights and transcriptional analysis of two

soluble di-iron monooxygenase genes. Front Microbiol 6:393. https://doi.org/10.3389/fmicb.2015.00393.
25. Krishnamoorthy G, Kaiser P, Lozza L, Hahnke K, Mollenkopf H-J, Kaufmann SHE. 2019. Mycofactocin is associated with ethanol metabolism in Mycobacteria. mBio 10:e00190-19. https://doi.org/10.1128/mBio.00190-19.
26. Barona-Gómez F, Lautru S, Francois-Xavier F, Leblond P, Pernodet JL, Challis GL. 2006. Multiple biosynthetic and uptake systems mediate siderophore-dependent iron acquisition in Streptomyces coelicolor A3(2) and Stremptomyces ambofaciens ATCC 23877. Microbiology (Reading) 152:3355–3366. https://doi.org/10.1099/mic.0.29161-0.
27. Ordóñez E, Thiyagarajan S, Cook JD, Stemmler TL, Gil JA, Mateos LM, Rosen BP. 2008. Evolution of metal(loid) binding sites in transcriptional regulators. J Biol Chem 283:25706–25714. https://doi.org/10.1074/jbc.M803209200.
28. Yoshinaga M, Rosen BP. 2014. A Cs^2As lyase for degradation of environmental organoarsenical herbicides and animal husbandry growth promoters. Proc Natl Acad Sci U S A 111:7701–7706. https://doi.org/10.1073/pnas.1403057111.
29. Chen J, Rosen BP. 2020. The arsenic methylation cycle: how microbial communities adapted methylarsenicals for use as weapons in the continuing war for dominance. Front Environ Sci 8:43. https://doi.org/10.3389/fenvs.2020.00043.
30. Retamal-Morales G, Mehnert M, Schwabe R, Tischler D, Zapata C, Chávez R, Schlömann M, Levicán G. 2018. Detection of arsenic-binding siderophores in arsenic-tolerating Actinobacteria by a modified CAS assay. Ecotoxicol Environ Saf 157:176–181. https://doi.org/10.1016/j.ecoenv.2018.03.087.
31. Bosello M, Zeyadi M, Kraas FI, Linne U, Xie X, Marahiel MA. 2013. Structural characterization of the heterobactin siderophores from Rhodococcus erythropolis PR4 and elucidation of their biosynthetic machinery. J Nat Prod 76:2282–2290. https://doi.org/10.1021/np4006579.
32. Johnstone TC, Nolan EM. 2015. Beyond iron: non-classical biological functions of bacterial siderophores. Dalton Trans 44:6320–6339. https://doi.org/10.1039/c4dt03559c.
33. Retamal-Morales G, Senges CHR, Stapf M, Olguín A, Modak B, Bandow JE, Tischler D, Schlömann M, Levicán G. 2021. Isolation and characterization of arsenic-binding siderophores from Rhodococcus erythropolis S43: role of heterobactin B and other heterobactin variants. Appl Microbiol Biotechnol 105:1731–1744. https://doi.org/10.1007/s00253-021-11123-2.
34. Birben E, Sahiner UM, Sackesen C, Erzurum S, Kalayci O. 2012. Oxidative stress and antioxidant defense. World Allergy Organ J 5:9–19. https://doi.org/10.1097/WOX.0b013e3182439613.
35. Castro-Severyn J, Pardo-Esté C, Mendez KN, Morales N, Marquez SL, Molina F, Remonsellez F, Castro-Nallar E, Saavedra CP. 2020. Genomic variation and arsenic tolerance emerged as niche specific adaptations by different Exiguobacterium strains isolated from the extreme Salar de Huasco environment in Chilean – Altiplano. Front Microbiol 11:1632. https://doi.org/10.3389/fmicb.2020.01632.
36. Sun D, Crowell SA, Harding CM, De Silva PM, Harrison A, Fernando DM, Mason KM, Santana E, Loewen PC, Kumar A, Liu Y. 2016. KatG and KatE confer Acinetobacter resistance to hydrogen peroxide but sensitize bacteria to killing by phagocytic respiratory burst. Life Sci 148:31–40. https://doi.org/10.1016/j.lfs.2016.02.015.
37. Carpenter BM, Whitmire JM, Merrell DS. 2009. This is not your mother's repressor: the complex role of Fur in pathogenesis. Infect Immun 77:2590–2601. https://doi.org/10.1128/IAI.00116-09.
38. LeBlanc JC, Gonçalves ER, Mohn WW. 2008. Global response to desiccation stress in the soil actinomycete Rhodococcus jostii RHA1. Appl Environ Microbiol 74:2627–2636. https://doi.org/10.1128/AEM.02711-07.
39. Fernandez NL, Waters CM. 2019. Cyclic di-GMP increases catalase production and hydrogen peroxide tolerance in vibrio cholerae. Appl Environ Microbiol 85:e01043-19. https://doi.org/10.1128/AEM.01043-19.
40. Sardiwal S, Kendall SL, Movahedzadeh F, Rison SCG, Stoker NG, Djordjevic S. 2005. A GAF domain in the hypoxia/NO-inducible Mycobacterium tuberculosis DosS protein binds haem. J Mol Biol 353:929–936. https://doi.org/10.1016/j.jmb.2005.09.011.
41. Huang C-J, Wang Z-C, Huang H-Y, Huang H-D, Peng H-L. 2013. YjcC, a c-di-GMP phosphodiesterase protein, regulates the oxidative stress response and virulence of Klebsiella pneumoniae CG43. PLoS One 8:e66740. https://doi.org/10.1371/journal.pone.0066740.
42. Ramírez-Díaz MI, Díaz-Pérez C, Vargas E, Riveros-Rosas H, Campos-García J, Cervantes C. 2008. Mechanisms of bacterial resistance to chromium compounds. Biometals 21:321–332. https://doi.org/10.1007/s10534-007-9121-8.
43. Crew R, Ramirez MV, England K, Slayden RA. 2015. MadR1, a Mycobacterium tuberculosis cell cycle stress response protein that is a member of a widely conserved protein class of prokaryotic, eukaryotic and archaeal origin. Tuberculosis (Edinb) 95:251–258. https://doi.org/10.1016/j.tube.2015.03.005.
44. Lee WL, Gold B, Darby C, Brot N, Jiang X, De Carvalho LPS, Wellner D, St John GWRJ, Jr, Nathan C. 2009. Mycobacterium tuberculosis expresses methionine sulphoxide reductases A and B that protect from killing by nitrite and hypochlorite. Mol Microbiol 71:583–593. https://doi.org/10.1111/j.1365-2958.2008.06548.x.
45. Kieser KJ, Rubin EJ. 2014. How sisters grow apart: mycobacterial growth and division. Nat Rev Microbiol 12:550–562. https://doi.org/10.1038/nrmicro3299.
46. Striebel F, Imkamp F, Özcelik D, Weber-Ban E. 2014. Pupylation as a signal for proteasomal degradation in bacteria. Biochim Biophys Acta 1843:103–113. https://doi.org/10.1016/j.bbamcr.2013.03.022.
47. Fay A, Glickman MS. 2014. An essential nonredundant role for mycobacterial DnaK in native protein folding. PLoS Genet 10:e1004516. https://doi.org/10.1371/journal.pgen.1004516.
48. Peña-Ortiz L, Graça AP, Guo H, Braga D, Köllner TG, Regestein L, Beemelmanns C, Lackner G. 2020. Structure elucidation of the redox cofactor mycofactocin reveals oligo-glycosylation by MftF. Chem Sci 11:5182–5190. https://doi.org/10.1039/d0sc01172j.
49. Reyes AM, Pedre B, De Armas MI, Tossounian MA, Radi R, Messens J, Trujillo M. 2018. Chemistry and redox biology of mycothiol. Antioxid Redox Signal 28:487–504. https://doi.org/10.1089/ars.2017.7074.
50. Dosanjh M, Newton GL, Davies J. 2008. Characterization of a mycothiol ligase mutant of Rhodococcus jostii RHA1. Res Microbiol 159:643–650. https://doi.org/10.1016/j.resmic.2008.08.006.
51. Borodina I, Kenny LC, McCarthy CM, Paramasivan K, Pretorius E, Roberts TJ, van der Hoek SA, Kell DB. 2020. The biology of ergothioneine, an antioxidant nutraceutical. Nutr Res Rev 33:190–217. https://doi.org/10.1017/S0954422419000301.
52. Rawat M, Av-Gay Y. 2007. Mycothiol-dependent proteins in actinomycetes. FEMS Microbiol Rev 31:278–292. https://doi.org/10.1111/j.1574-6976.2006.00062.x.
53. Cumming BM, Chinta KC, Reddy VP, Steyn AJC. 2018. Role of ergothioneine in microbial physiology and pathogenesis. Antioxid Redox Signal 28:431–444. https://doi.org/10.1089/ars.2017.7300.
54. Akanmu D, Cecchini R, Aruoma OI, Halliwell B. 1991. The antioxidant action of ergothioneine. Arch Biochem Biophys 288:10–16. https://doi.org/10.1016/0003-9861(91)90158-f.
55. Chen J, Yoshinaga M, Garbinski LD, Rosen BP. 2016. Synergistic interaction of glyceraldehydes-3-phosphate dehydrogenase and ArsJ, a novel organoarsenical efflux permease, confers arsenate resistance. Mol Microbiol 100:945–953. https://doi.org/10.1111/mmi.13371.
56. Zhang HN, Yang L, Ling JY, Czajkowsky DM, Wang JF, Zhang XW, Zhou YM, Ge F, Yang MK, Xiong Q, Guo SJ, Le HY, Wu SF, Yan W, Liu B, Zhu H, Chen Z, Tao SC. 2015. Systematic identification of arsenic-binding proteins reveals that hexokinase-2 is inhibited by arsenic. Proc Natl Acad Sci U S A 112:15084–15089. https://doi.org/10.1073/pnas.1521316112.
57. Nakayama T, Yonekura S-I, Yonei S, Zhang-Akiyama Q-M. 2013. Escherichia coli pyruvate:flavodoxin oxidoreductase, YdbK—regulation of expression and biological roles in protection against oxidative stress. Genes Genet Syst 88:175–188. https://doi.org/10.1266/ggs.88.175.
58. Li S, Ye Z, Moreb EA, Hennigan JN, Castellanos DB, Yang T, Lynch MD. 2021. Dynamic control over feedback regulatory mechanisms improves NADPH flux and xylitol biosynthesis in engineered E. coli. Metab Eng 64:26–40. https://doi.org/10.1016/j.ymben.2021.01.005.
59. Paul BD, Snyder SH. 2010. The unusual amino acid L-ergothioneine is a physiologic cytoprotectant. Cell Death Differ 17:1134–1140. https://doi.org/10.1038/cdd.2009.163.
60. Hernández MA, Mohn WW, Martínez E, Rost E, Alvarez AF, Alvarez HM. 2008. Biosynthesis of storage compounds by Rhodococcus jostii RHA1 and global identification of genes involved in their metabolism. BMC Genomics 9:600–614. https://doi.org/10.1186/1471-2164-9-600.
61. Maurya RK, Bharti S, Krishnan MY. 2018. Triacylglycerols: fuelling the hibernating Mycobacterium tuberculosis. Front Cell Infect Microbiol 8:450. https://doi.org/10.3389/fcimb.2018.00450.
62. Arora N, Gulati K, Patel A, Pruthi PA, Poluri KM, Pruthi V. 2017. A hybrid approach integrating arsenic detoxification with biodiesel production using oleaginous microalgae. Algal Res 24:29–39. https://doi.org/10.1016/j.algal.2017.03.012.
63. Cook GM, Hards K, Vilchèze C, Hartman T, Berney M. 2014. Energetics of respiration and oxidative phosphorylation in mycobacteria. Microbiol Spectr 2:MGM2-0015-2013. https://doi.org/10.1128/microbiolspec.MGM2-0015-2013.
64. Wiseman B, Nitharwal RG, Fedotovskaya O, Schäfer J, Guo H, Kuang Q, Benlekbir S, Sjöstrand D, Ädelroth P, Rubinstein JL, Brzezinski P, Högbom M. 2018. Structure of a functional obligate complex III2IV2 respiratory supercomplex from Mycobacterium smegmatis. Nat Struct Mol Biol 25:1128–1136. https://doi.org/10.1038/s41594-018-0160-3.

65. Berney M, Cook GM. 2010. Unique flexibility in energy metabolism allows mycobacteria to combat starvation and hypoxia. PLoS One 5:e8614. https://doi.org/10.1371/journal.pone.0008614.
66. Cordero PRF, Bayly K, Leung PM, Huang C, Islam ZF, Schittenhelm RB, King GM, Greening C. 2019. Atmospheric carbon monoxide oxidation is a widespread mechanism supporting microbial survival. ISME J 13:2868–2881. https://doi.org/10.1038/s41396-019-0479-8.
67. Berney M, Greening C, Hards K, Collins D, Cook GM. 2014. Three different [NiFe] hydrogenases confer metabolic flexibility in the obligate aerobe Mycobacterium smegmatis. Environ Microbiol 16:318–330. https://doi.org/10.1111/1462-2920.12320.
68. Sone N, Fukuda M, Katayama S, Jyoudai A, Syugyou M, Noguchi S, Sakamoto J. 2003. QcrCAB operon of a nocardia-form actinomycete Rhodococcus rhodochrous encodes cytochrome reductase complex with diheme cytochrome cc subunit. Biochim Biophys Acta Bioenerg 1557:125–131. https://doi.org/10.1016/S0005-2728(02)00394-8.
69. Kishikawa J, Kabashima Y, Kurokawa T, Sakamoto J. 2010. The cytochrome bcc-aa3-type respiratory chain of Rhodococcus rhodochrous. J Biosci Bioeng 110:42–47. https://doi.org/10.1016/j.jbiosc.2009.12.006.
70. Collins MD, Jones D. 1981. Distribution of isoprenoid quinone structural types in bacteria and their taxonomic implication. Microbiol Rev 45:316–354. https://doi.org/10.1128/mr.45.2.316-354.1981.
71. Pecsi I, Hards K, Ekanayaka N, Berney M, Hartman T, Jacobs WR, Cook GM. 2014. Essentiality of succinate dehydrogenase in Mycobacterium smegmatis and its role in the generation of the membrane potential under hypoxia. mBio 5:e01093-14. https://doi.org/10.1128/mBio.01093-14.
72. Zhang Y, Chen S, Hao X, Su J-Q, Xue X, Yan Y, Zhu Y-G, Ye J. 2016. Transcriptomic analysis reveals adaptive responses of an enterobacteriaceae strain LSJC7 to arsenic exposure. Front Microbiol 7:636. https://doi.org/10.3389/fmicb.2016.00636.
73. Tan MP, Sequeira P, Lin WW, Phong WY, Cliff P, Ng SH, Lee BH, Camacho L, Schnappinger D, Ehrt S, Dick T, Pethe K, Alonso S. 2010. Nitrate respiration protects hypoxic Mycobacterium tuberculosis against acid- and reactive nitrogen species stresses. PLoS One 5:e13356. https://doi.org/10.1371/journal.pone.0013356.
74. Sabaty M, Avazeri C, Pignol D, Vermeglio A. 2001. Characterization of the reduction of selenate and tellurite by nitrate reductases. Appl Environ Microbiol 67:5122–5126. https://doi.org/10.1128/AEM.67.11.5122-5126.2001.
75. Bailly X, Vanin S, Chabasse C, Mizuguchi K, Vinogradov SN. 2008. A phylogenomic profile of hemerythrins, the nonheme diiron binding respiratory proteins. BMC Evol Biol 8:244. https://doi.org/10.1186/1471-2148-8-244.
76. French CE, Bell JML, Ward FB. 2008. Diversity and distribution of hemerythrin-like proteins in prokaryotes. FEMS Microbiol Lett 279:131–145. https://doi.org/10.1111/j.1574-6968.2007.01011.x.
77. Nocek B, Kochinyan S, Proudfoot M, Brown G, Evdokimova E, Osipiuk J, Edwards AM, Savchenko A, Joachimiak A, Yakunin AF. 2008. Polyphosphate-dependent synthesis of ATP and ADP by the family-2 polyphosphate kinases in bacteria. Proc Natl Acad Sci U S A 105:17730–17735. https://doi.org/10.1073/pnas.0807563105.
78. Presentato A, Cappelletti M, Sansone A, Ferreri C, Piacenza E, Demeter MA, Crognale S, Petruccioli M, Milazzo G, Fedi S, Steinbüchel A, Turner RJ, Zannoni D. 2018. Aerobic growth of Rhodococcus aetherivorans BCP1 using selected naphthenic acids as the sole carbon and energy sources. Front Microbiol 9:672. https://doi.org/10.3389/fmicb.2018.00672.
79. Seufferheld MJ, Alvarez HM, Farias ME. 2008. Role of polyphosphates in microbial adaptation to extreme environments. Appl Environ Microbiol 74:5867–5874. https://doi.org/10.1128/AEM.00501-08.
80. Langmead B, Salzberg SL. 2012. Fast gapped-read alignment with Bowtie 2. Nat Methods 9:357–359. https://doi.org/10.1038/nmeth.1923.
81. Hilker R, Stadermann KB, Doppmeier D, Kalinowski J, Stoye J, Straube J, Winnebald J, Goesmann A. 2014. ReadXplorer—visualization and analysis of mapped sequences. Bioinformatics 30:2247–2254. https://doi.org/10.1093/bioinformatics/btu205.
82. Love MI, Huber W, Anders S. 2014. Moderated estimation of fold change and dispersion for RNA-seq data with DESeq2. Genome Biol 15:550–521. https://doi.org/10.1186/s13059-014-0550-8.
83. Huerta-Cepas J, Szklarczyk D, Heller D, Hernández-Plaza A, Forslund SK, Cook H, Mende DR, Letunic I, Rattei T, Jensen LJ, Von Mering C, Bork P. 2019. EggNOG 5.0: a hierarchical, functionally and phylogenetically annotated orthology resource based on 5090 organisms and 2502 viruses. Nucleic Acids Res 47:D309–D314. https://doi.org/10.1093/nar/gky1085.
84. Blin K, Shaw S, Kloosterman AM, Charlop-Powers Z, van Wezel GP, Medema MH, Weber T. 2021. antiSMASH 6.0: improving cluster detection and comparison capabilities. Nucleic Acids Res 49:W29–W35. https://doi.org/10.1093/nar/gkab335.